NUREG/CR–4273
IS–4878

Crack Propagation in High Strain Regions of Sequoyah Containment

Prepared by:
L. Greimann, F. Fanous, D. Bluhm

Ames Laboratory
Iowa State University

Prepared for
U.S. Nuclear Regulatory Commission

AVAILABILITY NOTICE

Availability of Reference Materials Cited in NRC Publications

Most documents cited in NRC publications will be available from one of the following sources:

1. The NRC Public Document Room, 2120 L Street, NW., Lower Level, Washington, DC 20555

2. The Superintendent of Documents, U.S. Government Printing Office, P.O. Box 37082, Washington, DC 20013-7082

3. The National Technical Information Service, Springfield, VA 22161

Although the listing that follows represents the majority of documents cited in NRC publications, it is not intended to be exhaustive.

Referenced documents available for inspection and copying for a fee from the NRC Public Document Room include NRC correspondence and internal NRC memoranda; NRC bulletins, circulars, information notices, inspection and investigation notices; licensee event reports; vendor reports and correspondence; Commission papers; and applicant and licensee documents and correspondence.

The following documents in the NUREG series are available for purchase from the GPO Sales Program: formal NRC staff and contractor reports, NRC-sponsored conference proceedings, international agreement reports, grant publications, and NRC booklets and brochures. Also available are regulatory guides, NRC regulations in the *Code of Federal Regulations*, and *Nuclear Regulatory Commission Issuances*.

Documents available from the National Technical Information Service include NUREG-series reports and technical reports prepared by other Federal agencies and reports prepared by the Atomic Energy Commission, forerunner agency to the Nuclear Regulatory Commission.

Documents available from public and special technical libraries include all open literature items, such as books, journal articles, and transactions. *Federal Register* notices, Federal and State legislation, and congressional reports can usually be obtained from these libraries.

Documents such as theses, dissertations, foreign reports and translations, and non-NRC conference proceedings are available for purchase from the organization sponsoring the publication cited.

Single copies of NRC draft reports are available free, to the extent of supply, upon written request to the Office of Administration, Distribution and Mail Services Section, U.S. Nuclear Regulatory Commission, Washington, DC 20555.

Copies of industry codes and standards used in a substantive manner in the NRC regulatory process are maintained at the NRC Library, 7920 Norfolk Avenue, Bethesda, Maryland, for use by the public. Codes and standards are usually copyrighted and may be purchased from the originating organization or, if they are American National Standards, from the American National Standards Institute, 1430 Broadway, New York, NY 10018.

DISCLAIMER NOTICE

NUREG/CR–4273
IS–4878

Crack Propagation in High Strain Regions of Sequoyah Containment

Prepared by:
L. Greimann, F. Fanous, D. Bluhm

Ames Laboratory
Iowa State University

Prepared for
U.S. Nuclear Regulatory Commission

AVAILABILITY NOTICE

Availability of Reference Materials Cited in NRC Publications

Most documents cited in NRC publications will be available from one of the following sources:

1. The NRC Public Document Room, 2120 L Street, NW., Lower Level, Washington, DC 20555

2. The Superintendent of Documents, U.S. Government Printing Office, P.O. Box 37082, Washington, DC 20013-7082

3. The National Technical Information Service, Springfield, VA 22161

Although the listing that follows represents the majority of documents cited in NRC publications, it is not intended to be exhaustive.

Referenced documents available for inspection and copying for a fee from the NRC Public Document Room include NRC correspondence and internal NRC memoranda; NRC bulletins, circulars, information notices, inspection and investigation notices; licensee event reports; vendor reports and correspondence; Commission papers; and applicant and licensee documents and correspondence.

The following documents in the NUREG series are available for purchase from the GPO Sales Program: formal NRC staff and contractor reports, NRC-sponsored conference proceedings, international agreement reports, grant publications, and NRC booklets and brochures. Also available are regulatory guides, NRC regulations in the *Code of Federal Regulations*, and *Nuclear Regulatory Commission Issuances*.

Documents available from the National Technical Information Service include NUREG-series reports and technical reports prepared by other Federal agencies and reports prepared by the Atomic Energy Commission, forerunner agency to the Nuclear Regulatory Commission.

Documents available from public and special technical libraries include all open literature items, such as books, journal articles, and transactions. *Federal Register* notices, Federal and State legislation, and congressional reports can usually be obtained from these libraries.

Documents such as theses, dissertations, foreign reports and translations, and non-NRC conference proceedings are available for purchase from the organization sponsoring the publication cited.

Single copies of NRC draft reports are available free, to the extent of supply, upon written request to the Office of Administration, Distribution and Mail Services Section, U.S. Nuclear Regulatory Commission, Washington, DC 20555.

Copies of industry codes and standards used in a substantive manner in the NRC regulatory process are maintained at the NRC Library, 7920 Norfolk Avenue, Bethesda, Maryland, for use by the public. Codes and standards are usually copyrighted and may be purchased from the originating organization or, if they are American National Standards, from the American National Standards Institute, 1430 Broadway, New York, NY 10018.

NUREG/CR–4273
IS–4878

Crack Propagation in High Strain Regions of Sequoyah Containment

Manuscript Completed: July 1985
Date Published: March 1993

Prepared by
L. Greimann, F. Fanous, D. Bluhm

Ames Laboratory
Iowa State University
Ames, IA 50011

Prepared for
Division of Engineering
Office of Nuclear Reactor Regulation
U.S. Nuclear Regulatory Commission
Washington, DC 20555
NRC FIN A4136

ABSTRACT

The rate of release of radiooctive materials from a containment during a severe accident has a significant impact on the consequences of the accident. One hypothesis for a containment leakage model states that the containment will develop a controlled, relatively small leak before the pressure reaches the point where a general rupture of the shell occurs. Another states that overall failure will occur with total release of the vessel contents almost instantaneously. The Sequoyah ice condenser containment vessel has been studied for some time to predict the possible location and extent of leakage which could occur during a severe accident. In this work, three critical high strain locations were studied to predict crack propagation from an initially small defect.

The 1/2-inch plate near the Sequoyah springline was selected for further study. A detailed finite element model of the region was prepared and a virtual crack extension method for calculating the J integral was developed for use with the general purpose finite element program. The pressure in the model was increased to 78 psi which produced a maximum membrane strain of 6.5 percent. At this point the surface crack was assumed to propagate through the plate and leakage began. Using the virtual crack extension method, two through cracks with different lengths were found to be unstable at this pressure which would allow almost instantaneous release of the vessel contents.

TABLE OF CONTENTS

LIST OF TABLES

LIST OF FIGURES

ACKNOWLEDGMENT

The authors would like to express their appreciation to three members of the U.S. Nuclear Regulatory Commission, Mr. Goutam Bagchi, Leader, Seismic Qualification Section; Mr. James Knight, Acting Director, Division of Engineering; and Mr. Robert Wright, NRC Project Manager, Division of Engineering, for their help throughout the course of this work. The authors also wish to acknowledge the able assistance of the Project Secretaries, Connie Bates and Beth Lott, for the word processor operations and secretarial services associated with this project.

EXECUTIVE SUMMARY

The rate of release of radioactive materials from a containment during a severe accident has a significant impact on the consequences of the accident. One hypothesis for a containment leakage model states that the containment will develop a controlled, relatively small leak before the pressure reaches the point where a general rupture of the shell occurs. Another hypothesis states that an overall failure will occur with total release of the vessel contents almost instantaneously. As part of the Containment Performance Working Group (CPWG) and other studies, the Sequoyah ice condenser containment vessel has been studied for some time to predict the possible location and extent of leakage which could occur during a severe accident. In this work, three critical high strain locations were studied to predict crack propagation from an initially small defect.

Several criteria are presented in the literature for predicting crack growth in highly ductile materials such as containment steels. The J integral approach is adopted herein. In simple idealized cases, the J-applied value is given by curve-fits of numerical results that have been developed by others. In this work, a virtual crack extension method for calculating J has been developed for use with a general purpose finite element programs. The various methods are compared herein. Approximate values of the material J-resistance are tabulated.

An initially small surface flaw is first postulated in each of the critical high strain regions. By comparing the J-applied value to the J-resistance, the pressure at which this surface crack propagates is estimated for each of these regions. The 1/2-inch plate near the Sequoyah springline is then selected for further study. A detailed finite element model of the region was prepared and analyzed with the ANSYS program. The pressure in the model was increased up to 78 psi which produced a maximum membrane strain of 6.5 percent. At this point the surface crack was assumed to propagate through the plate and leakage began. Using the virtual crack extension method, two through cracks with different lengths were found to be unstable at this pressure.

If the critical membrane strain is about 6.5 percent, the Sequoyah containment vessel will begin to leak at about 78 psi. The resulting through crack will not be stable and general failure will occur with the almost instantaneous release of the vessel contents.

1. INTRODUCTION

During a severe accident, a containment may develop a controlled, relatively small, leak before the pressure reaches the point where a general rupture of the shell occurs. On the other hand, overall failure may occur with total instantaneous release of the vessel contents. Either possibility may occur, depending primarily upon local geometry, material details and the applied pressure [1.1].

The NRC has established a Containment Performance Working Group (CPWG) at the request of the Severe Accident Research Plan (SARP) Senior Review Group to study several models of containment leakage. The members of this group have studied many possible leak models [1.2] such as pre-existing leakage, hatch seals, general rupture and flange opening. For many of the containments it was quite clear where leakage would first occur. However, even though the Sequoyah containment vessel (Fig. 1.1) has been carefully studied for the past several years [1.3, 1.4], it is not clear what is the weakest point in this vessel.

Containment Shell - The containment shell is estimated to have a strength at which "significant yielding" occurs between 55 and 60 psi [1.5]. This strength is controlled by the 1/2-inch plate near the springline. The design pressure is 12 psi.

Penetrations - A study of all the penetrations in the Sequoyah containment, using plastic collapse mechanism equations, indicates that the weakest penetration is at Elev. 767', AZ 266° [1.3].

Equipment Hatch Seal - The most recent Sequoyah study [1.6] investigated leakage of the equipment hatch seal as the containment shell deforms the penetration sleeve. The three-dimensional finite element model indicated that relative motion of the flange interfaces was not sufficient to permit leakage at 82 psi.

If a through crack develops at any of these high strain locations (and, possibly, several others), leakage will begin. The amount of leakage will depend upon how far the crack extends. For example, a crack in the 1/2-inch containment plate, Fig. 1.2, may be arrested by an adjacent stiffener or the adjacent thicker plate; or, it may propagate through both of these. In this and other regions, the high strains may be sufficiently localized so that the crack arrests as it moves from the region.

1.1 Objective

The objective of this work is to predict the extent of crack propagation which will occur from a postulated small crack in the high strain regions of the Sequoyah containment.

1.2 Approach

The general approach to studying this problem is, first, to select a crack growth criteria from the current state-of-the-art of the elastic-plastic fracture mechanics field--the J integral. The analytical tools required to calculate the J integral and the experimental data required to characterize the material J resistance are summarized next. After postulating an initial surface flaw, the growth criteria is applied to predict when a through crack develops and how far the through crack extends.

1.3 References

1.1 Kussmaul, K., et. al, "Crack Arrest Behavior in Pressure Vessels," Paper B/F 4/10, SMIRT, August 1983, pp. 337-346.

1.2 Containment Performance Working Group, "Containment Leak Rate Estimates," Fourth Draft, NUREG/1037, March 1984.

1.3 Greimann, L., Fanous, F. and Bluhm, D., "Reliability Analysis of Containment Strength," NUREG/CR-1891, August 1982.

1.4 ACRS, Subcommittee on Structural Engineering, "Establishing the Maximum Internal Pressure that the Sequoyah Containment Structure Can Withstand," Washington, D.C., September 2, 1980.

1.5 Greimann, L., Fanous, F., and Bluhm, D., "Containment Analysis Techniques, A State-of-the-Art Summary," NUREG/CR-3653, March 1984.

1.6 Greimann, L., Fanous, F., and Bluhm, D., "Sequoyah Equipment Hatch Seal Leakage," NUREG/CR-3952, IS-3952, Final Report, February 1985.

2. CRACK GROWTH CRITERIA

2.1 Crack Growth Process

For the nuclear containment leakage considered here, the crack will be assumed to begin as a partially-through surface crack of approximately elliptical shape. Figure 2.1 shows such a crack (Fig. 2.1a) in a flat plate (Fig. 2.1d) subjected to a uniaxial stress, σ. As the stress is increased, the crack is visualized as first propagating through the thickness B (Fig. 2.1b). Leakage begins at this point. The extent of leakage is controlled by how far the through crack (Fig. 2.1c) propagates across the plate.

2.2 Review of Criteria

There are no crack growth criteria for ductile materials which are generally accepted by the fracture mechanics community. No single parameter or combination of parameters have been found which satisfactorily characterize the growth of cracks through regions of high strain and with gross plasticity of highly ductile materials. Currently, the state-of-the-art in fracture mechanics permits the reliable prediction of small crack growths in regions of limited plasticity. It is beyond the scope of this work to review completely the state-of-the-art in elastic-plastic fracture mechanics (EPFM). Indeed, the authors are not qualified to make the judgments necessary for such a review. However, a very brief listing of the various criteria is justified.

J Integral. The J integral is a measure of the energy release rate as a crack extends. This approach has become popular in the United States for nuclear reactor vessels [2.1, 2.2, 2.3, 2.4, 2.5, 2.6, 2.7, 2.8].

CTOD. The crack tip opening displacement (CTOD) hypothesis states that a crack will grow when the opening near the crack tip reaches a critical value [2.3, 2.4, 2.6, 2.7].

Modified R-6 Assessment Diagram. This approach, which is popular in the United Kingdom, presents an interaction type equation between the extreme limits of crack extension in a perfectly elastic material (brittle fracture) and plastic collapse governed by a limit load [2.9, 2.10, 2.11, 2.12].

Crack Tip Energy Release Rate. Probably related to the J integral approach, the crack tip energy release rate criterion considers the amount of plastic energy in the immediate vicinity of the crack tip [2.13].

Strain Energy Density. In the strain energy density criterion, the crack is assumed to grow when the strain energy density immediately ahead of the crack reaches a critical value which can be obtained from a uniaxial tensile test [2.14, 2.15, 2.16, 2.17, 2.18].

Each of these criteria has its proponents. They have been reviewed by experts in the fracture mechanics field and compared [2.10, 2.11, 2.19, 2.20, 2.21, 2.22]. Each has an area of application and, yet, none is completely satisfactory for the complete description of ductile crack growth. If the number of proponents can be used as a legitimate measure of the validity of the criterion, the J integral and CTOD approaches are more accepted [2.10, 2.21]. The J integral criteria will be adopted herein.

2.3 J Controlled Crack Growth

The J integral has been defined in a number of ways but perhaps the most physically appealing way is to define J as the generalized force associated with an increment of crack growth. The energy balance equations for an increment of crack area δA is

$$J\,\delta A + \delta U + \delta V = 0 \tag{2.1}$$

where

$$\delta U = \delta \int_V W dv \tag{2.2}$$

$$W = \int_0^{\varepsilon} \sigma d\varepsilon \tag{2.3}$$

is the increment in internal strain energy for the increment in strain $\delta\varepsilon$ which is associated with the δA growth. The quantity W is the strain energy density. The quantity,

$$\delta V = - F\,\delta u \tag{2.4}$$

is the increment in external energy for the increment in displacement δu associated with δA. The first term in Eq. 2.1 is the energy required to form the new crack with a surface area of δA. The applied J integral can be calculated in a number of ways, as will be discussed in Section 2.4. Crack growth is presumed to occur when J reaches some critical value J_R, usually considered to be a material property. The J_R resistance is usually characterized by the J_R vs. Δa curve (Fig. 2.3) where Δa is an increment in length of crack growth. Hence, crack growth occurs if

$$J > J_R \tag{2.5}$$

The amount of growth is controlled by the J_R curve. The J criteria applies to a limited amount of growth [2.1, 2.4, 2.5, 2.7]:

$$C >> \begin{cases} J_R/\sigma_y \\ J_R / \left(\dfrac{dJ_R}{da}\right) \end{cases} \tag{2.6}$$

where C is the remaining ligament, i.e., the remaining portion of the material ahead of the crack tip (Fig. 2.2).

2.4 J - Applied

2.4.1 Crack Idealization and Elastic Solutions

As shown in Fig. 2.1, two crack shapes are envisioned as the crack grows--an initial surface crack and a through crack. The surface crack can probably best be idealized as an eliptic crack. However, there are limited plastic solutions for this crack shape. If the crack is long ($a << c$), the conditions at the base of the crack are approximated by a single edge cracked plate under tension (ECPT) in plane strain. After the crack has propagated through the plate, the conditions approximate a center cracked plate (CCP) in plane stress. For these conditions, the elastic solution for J can be written as [2.7]

$$J_e = \frac{Y^2 \pi \sigma^2 a}{E} \tag{2.7}$$

in which

$$Y = \begin{cases} 1.12\sqrt{1-\nu^2} & \text{ECPT} \\ \sqrt{\sec\frac{\pi a}{W}} & \text{CCP} \end{cases}$$

The above solution for the ECPT case is limited to shallow cracks ($a << B$).

2.4.2 Analytic Elastic-Plastic Solutions

The application of J in the nonlinear range depends upon the calculation of J and this has been the subject of many studies--both analytical and numerical (finite element). Here, we will summarize a few solutions which seem to attract the most attention. Most of these solutions use a Ramberg-Osgood approximation to the true stress-true strain curve from a uniaxial tensile test of the material:

$$\frac{\varepsilon}{\varepsilon_y} = \frac{\sigma}{\sigma_y} + \alpha \left(\frac{\sigma}{\sigma_y}\right)^n \tag{2.8}$$

in which σ_y and ε_y are the material true yield stress and strain, respectively, and α and n are material constants which are selected to provide a good fit to the experimental curve [2.20]. For purposes of presentation, the yield J will be defined by

$$J_y = \frac{Y^2 \pi \sigma_y^2 a}{E} \tag{2.9}$$

Turner [2.19, 2.22] gives, perhaps, the simplest approximation to J as

$$\frac{J}{J_y} = \begin{cases} \left(\frac{\varepsilon}{\varepsilon_y}\right)^2 \left[1 + 0.5\left(\frac{\varepsilon}{\varepsilon_y}\right)^2\right] & \frac{\varepsilon}{\varepsilon_y} < 1.2 \\ 2.5\left(\frac{\varepsilon}{\varepsilon_y} - 0.2\right) & \frac{\varepsilon}{\varepsilon_y} > 1.2 \end{cases} \qquad (2.10)$$

This approximation is intended to be an upper bound to most practical cases, including surface and through cracks. The above equation does not include a correction for deep notches which Turner has suggested.

Paris [2.1] has presented an equation for surface and through cracks in A533 steel for the ductile range as

$$\frac{J}{J_y} = \frac{1}{\pi} \begin{cases} 3.3\left(\frac{\sigma}{\sigma_y}\right)^2 + 3.14\ \alpha\ \left(\frac{\sigma}{\sigma_y}\right)^{n+1} & \text{Surface} \\ 4.3\left(\frac{\sigma}{\sigma_y}\right)^2 + 10.6\ \alpha\ \left(\frac{\sigma}{\sigma_y}\right)^{n+1} & \text{Through} \end{cases} \qquad (2.11)$$

After several years of study, the EPRI [2.2, 2.3, 2.4, 2.23] presents J solutions as the sum of the elastic and fully-plastic cases

$$\frac{J}{J_y} = \left(\frac{\sigma}{\sigma_y}\right)^2 + \frac{\alpha\ h_1\ c}{\pi\ b\ Y^2}\left(\frac{P}{P_y}\right)^{n+1} \qquad (2.12)$$

in which the notation is as follows:

		ECPT	CCP
c (net width)	=	b - a	W/2 - a
b (total width)	=	B	W/2
P (load)	=	σB	σW
P_y (limit load)	=	$1.46\ \sigma_y\left[\left(c^2+a^2\right)^{1/2} - a\right]$	$\sigma_y(W-2a)$
$h_1\left(\frac{a}{b} = \frac{1}{8}\right)$	=	21.7	4.62
$h_1\left(\frac{a}{b} = \frac{1}{4}\right)$	=	3.02	2.86
Y	=	$\frac{P_y}{\sigma_y B}$	$\frac{P_y}{\sigma_y W}$

In this equation, h_1 is dependent upon the specimen shape, crack size, and material shape parameter n. It has been obtained for several cases by EPRI using numerical methods for the fully plastic solutions. The values tabulated above are for a shape factor n = 10. The solution for the plane strain ECPT case are from [2.23] (not [2.4]) and for the plane stress CCP are from [2.4]. The EPRI correction for effective crack length in the elastic portion has not been included.

A modified form of the R-6 assessment diagram has been suggested by Chell and Milne [2.10] and is given by a parametric equation as

$$\frac{J}{J_y} = \frac{8}{\pi^2 \gamma} \ln \sec \frac{\pi}{2} \rho$$

$$\frac{P}{P_y} = \left[\rho + \left(1 - \sqrt[4]{\frac{J_y \rho^2}{J}}\right)\left(\frac{\sigma_u}{\sigma_y} - 1\right)\right] \frac{(1 + \sigma_u/\sigma_y)}{2} \qquad (2.13)$$

in which the parameter ρ ranges as

$$0 \leq \rho < 1$$

and σ_u is the ultimate tensile stress. The term on the extreme right follows their suggestion to use a flow stress (arithmetic mean of the yield and ultimate) in the evaluation of the limit load. Equation 2.13 is plotted parametrically as ρ ranges from 0 to 1.

The above four solutions are plotted for a CCP case in Fig. 2.4. Note that, in order to plot the results on the strain abcissa, the Ramberg-Osgood relationship, Eq. 2.8, was used in conjunction with Eqs. 2.11, 2.12, and 2.13 to find the strain corresponding to any stress state.

2.4.3 Finite Element Elastic-Plastic Solutions

Most numerical solutions for the J integral are by one of two methods. In one method, the contour integral formulation of J is used directly [2.2, 2.3, 2.4, 2.7, 2.11, 2.23, 2.24, 2.25, 2.26, 2.27] by integrating along several paths around the crack tip. The virtual crack extension (VCE) method is a second popular method [2.6, 2.28, 2.29, 2.30, 2.31, 2.32, 2.33, 2.34]. The VCE method, which will be adopted here, basically uses the J definition in Eq. 2.1. The crack is given a virtual area growth δA. The virtual change in internal and external energy caused by this growth can be calculated. This is equal to the amount of surface energy released during the growth. The generalized force J can then be calculated directly by Eq. 2.1.

The virtual crack extension is usually accomplished by a series of stress free nodal shifts and releases as the crack propagates [2.3, 2.29, 2.30, 2.33, 2.34]. The virtual crack extension is accomplished

by a virtual change in the nodal coordinates (stress-free) with no total volume change and is not the same as a virtual displacement. Hence, in Fig. 2.5, node C is given a virtual stress-free coordinate shift of δa to C'. The nodes on the boundary are not permitted to move during this virtual change. (The location of the outer boundary is arbitrary but different J values will be obtained for each because: (1) J is not totally path independent for inelastic materials and (2) finite element mesh size will have a varying effect.) The virtual coordinate changes between C' and the boundary are usually taken to vary linearly [2.3].

To accomplish the virtual coordinate shift in an existing general purpose finite element program with a minimum of change, phantom elements are introduced. In the region depicted in Fig. 2.5, the phantom elements duplicate the real elements except they are connected to the node C'. The phantom elements are given a very small thickness, say 0.0001 times the real thickness. Hence, as the structure is loaded, these elements accumulate stress and strain, i.e., strain energy density. However, the strain energy is insignificant since their volume is very small. Suppose the structure with the real and phantom elements has been loaded to same load level at which the J calculation is desired. At this point, the crack is given a virtual crack extension, δa, that is, the phantom elements became real elements and vice versa. Since the boundary does not move, the change in external potential energy is zero and, using Eq. 2.1,

$$J = -\frac{1}{\delta A}\,\delta U \tag{2.14}$$

or, using Eq. 2.2,

$$J = -\frac{1}{\delta A}\left[\int_V \delta W\, dV + \int_{\delta V} W dV\right) \tag{2.15}$$

If, for example, the constant strain triangle finite element is used, i.e., W is constant within an element,

$$J = -\frac{1}{\Delta A}\left[\sum_{i}^{\text{elements}} (\sigma_i V_i \Delta\varepsilon_i + W_i \Delta V_i)\right] \tag{2.16}$$

in which σ_i, W_i and V_i are the stress, strain energy density and the volume of the real element i, respectively. The increments are

$$\Delta\varepsilon = \varepsilon_i' - \varepsilon_i \tag{2.17}$$

$$\Delta V_i = V_i' - V_i \tag{2.18}$$

where ε_i' denotes the strain in the phantom element corresponding to the real element i. The volume V_i' is the volume of phantom element using the real thickness, i.e.,

$$\Delta V_i = (A_i' - A_i)\, B_i \qquad (2.19)$$

where A_i' represents the area of the phantom element and A_i and B_i are the area and the thickness of the real element, respectively.

To check this approach and compare it to the analytical methods, it was applied to the CCP specimen in Fig. 2.6. The finite element idealization was analyzed with ANSYS [2.35]. (Note the crude mesh of constant strain triangles.) The virtual crack extension was 0.6 inch. Phantom elements duplicated the real elements in the lightly shaded area except node C was shifted up 0.6 inch.

First a static analysis procedure was tried. In this procedure, the applied edge stresses were increased in increments and a sufficient number of iterations were run to permit convergence. In the ANSYS program, convergence criteria are: (1) the charge in displacement between consecutive iterations must be less than 0.001 inch and, (2) the charge in plastic strain divided by the yield strain must be less than 0.01. It was found that the static analysis requires several hours of computer time even when these convergence criteria were relaxed somewhat.

To reach a converged solution using a reasonable number of iterations, the slow dynamic analysis procedure suggested in Ref. [2.35] was used. The dynamic solution within ANSYS permits an extrapolation procedure for plastic strains not available in the static solution. Hence, a converged solution can be obtained more rapidly using a dynamic solution. High damping was used to minimize the vibration response. Physically, this would correspond to placing the structure in a viscous fluid during the loading process. Mass-proportional damping was used to approximate the critically damped case. The fundamental frequency for the plate shown in Fig. 2.6 was estimated as 4300 rad./sec and, hence, the proportionality constant was taken as 8000/sec.

The applied edge stress was increased in steps. For each step, the applied stress was first increased over a rise time of one second, which is larger than several times the structure fundamental period. Next, the applied stress was held constant for several seconds. In each step a very small integration step size, Δt, was used (0.001 sec.). During the solution, Δt does not remain constant but changes automatically as optimized by the ANSYS program based on the third derivative of the displacement with respect to time (jerk).

The finite element results were used in conjunction with Eq. 2.14 to calculate J at different applied stress levels. This was accomplished using the ANSYS postprocesser and a computer program written by the authors. The calculated J for the CCP specimen in Fig. 2.6 are plotted in Fig. 2.4. For the elastic case (Linear Elastic Fracture Mechanics), the exact J for an applied nominal stress of 10 ksi is

$$J_e = 0.0636 \quad k\ in/in^2$$

The finite element procedure using phantom elements give

$$J_e = 0.0643 \quad k \text{ in/in}^2$$

which is certainly a favorable comparison considering the coarse mesh. As can be seen from Fig. 2.4, the proposed analysis gives results below the results predicted by Paris, EPRI and Turner in the high strain region (several times yield). This discrepancy is mostly caused by the coarse mesh around the crack.

2.5 J-Resistance

As in Eq. 2.5 and Fig. 2.3, the resistance of the material to crack extension is characterized by the J resistance. The material in the Sequoyah containment is A516, Gr. 60 steel. Typical properties of the steel in this particular containment are listed in Table 2.1. (Note: these are "typical", i.e., from a very small sample and do not necessarily represent the mean values.) As usual, properties such as yield strength and Charpy values degrade with increasing thickness. No J_R values were available for this material when this study was conducted.

To establish an estimate of the J-resistance, similar steels were considered. Figure 2.7 is a plot of the Charpy value versus the J_{50} resistance, which is a measure of J-resistance defined by Paris [2.1] for reactor steel (A533B). Attempted correlations by Paris [2.1] and Kussmaul [2.8] are illustrated. Using a very gross extrapolation and the Charpy values in Table 2.1, one could estimate the J_{50} value to be in the range of 1 to 2 K in/in^2 for 3-inch plate and 3 to 6 K in/in^2 for 3/4-inch plate at -30° F. Data presented by Rolfe [2.36] for J versus Δa curves for structural steel and others [2.8, 2.37, 2.38] suggests that these values are, at least, the correct order of magnitude (Fig. 2.8).

For use in both the analytical and finite element analyses to follow, the stress-strain curve for the steel is idealized as in Fig. 2.9. The true stress-true strain curve approximates that found for the steel in much thinner plate [2.39]. The Ramberg-Osgood equation, Eq. 2.8, is used to approximate the true stress-true strain curve for the analytical J calculations. The piecewise linear, engineering strain curve is used in the finite element analysis.

2.6 References

2.1 Paris, P.C. and Johnson, R.E.," A Method of Application of Elastic-Plastic Fracture Mechanics to Nuclear Vessel Analysis," Elastic-Plastic Fracture: Second Symposium, Volume II - Fracture Resistance Curves and Engineering Applications, ASTM Special Technical Publication 803, October 1981, pp. II-5 to II-40.

2.2 Shih, C.F., Kumar, V. and German, M.D., "Studies of the Failure Assessment Diagram using the Estimation Method and J-Controlled Crack Growth Approach," Elastic-Plastic Fracture: Second Symposium, Volume II - Fracture Resistance Curves and Engineering Applications, ASTM Special Technical Publication 803, October 1981, pp. II-239 to II-261.

2.3 Kumar, V., et. al, Advances in Elastic-Plastic Fracture Analysis, Electric Power Research Institute, EPRI NP-3607, August 1984.

2.4 Kumar, V., German, M.D. and Shih, C.F., An Engineering Approach for Elastic-Plastic Fracture Analysis, Electric Power Research Institute, EPRI NP-1931, July 1981.

2.5 Ernst, H.A., "Material Resistance and Instability Beyond J-Controlled Crack Growth," Elastic-Plastic Fracture: Second Symposium, Volume I - Inelastic Crack Analysis, ASTM Special Technical Publication 803, October 1981, pp. I-191 to I-213.

2.6 de Lorenzi, H.G., "Elastic-Plastic Analysis of the Maximum Postulated Flaw in the Beltline Region of a Reactor Vessel," Aspects of Fracture Mechanics in Pressure Vessels and Piping, PVP-Vol. 58, ASME, July 1982, pp. 71-90.

2.7 Broek, D., Elementary Engineering Fracture Mechanics, Third Edition, Boston: Martinus Nijhoff, 1982.

2.8 Kussmaul, K., et. al, "Crack Arrest Behavior in Pressure Vessels," Paper G/F 4/10, SMIRT, August 1983, pp. 337-346.

2.9 Milne, I., "Calculating the Load Bearing Capacity of a Structure Failing by Ductile Crack Growth," Advances in Fracture Research, Proceedings of 5th International Conference on Fracture, Cannes, France, March 29-April 3, 1981, pp. 1751-1757.

2.10 Chell, G.G. and Milne, I., "Ductile Tearing Instability Analysis: A Comparison of Available Techniques," Elastic-Plastic Fracture: Second Symposium, Volume II - Fracture Resistance Curves and Engineering Applications, ASTM Special Technical Publication 803, October 1981, pp. II-179 to II-205.

2.11 Bloom, J.M., "Validation of a Deformation Plasticity Failure Assessment Diagram Approach to Flaw Evaluation," Elastic-Plastic Fracture: Second Symposium, Volume II - Fracture Resistance Curves and Engineering Applications, ASTM Special Technical Publication 803, October 1981, pp. II-206 to II-238.

2.12 Sarmiento, G.S., et. al, "Failure Internal Pressure of Spherical Steel Containments," Second Workshop on Containment Integrity, NUREG/CP-0056, August 1984.

2.13 Saka, M., et. al, "A Criterion Based on Crack-Tip Energy Dissipation in Plane-Strain Crack Growth Under Large-Scale Yielding," Elastic-Plastic Fracture: Second Symposium, Volume I - Inelastic Crack Analysis, ASTM Special Technical Publication 803, October 1981, pp. I-130 to I-158.

2.14 Sih, G.C., "Mechanics of Subcritical Crack Growth," Fracture Mechanics Technology Applied to Material Evaluation and Structure Design, The Hague: Marinus Nijhoff, 1983, pp. 3-18.

2.15 Sih, G.C. and Tzou, D.Y., "Mechanics of Nonlinear Crack Growth: Effects of Specimen Size and Loading Rate," Modeling Problems in Crack Tip Mechanics, University of Waterloo, Ontario, Canada, August 1983, pp. 155-169.

2.16 Carpinteri, A. and Sih, G.C., "Damage Accumulation and Crack Growth in Bilinear Materials with Softening: Application of Strain Energy Density Theory," Theoretical and Applied Fracture Mechanics. Vol. I, 1984, pp. 145-159.

2.17 Gdoutos, E.E., "Stable Growth of a Control Crack," Theoretical and Applied Fracture Mechanics, Vol. 1, 1984, pp. 139-144.

2.18 Sih, G.C. and Chang, C.I., "Prediction of Failure Sites Ahead of Moving Energy Source," Fracture Mechanics Technology Applied to Material Evaluation and Structure Design, The Hague: Marinus Nijhoff, 1983, pp. 171-187.

2.19 Turner, C.E., "Further Developments on a J-Based Design Curve and its Relationship to Other Procedures," Elastic-Plastic Fracture: Second Symposium, Volume II - Fracture Resistance Curves and Engineering Applications, ASTM Special Technical Publication 803, October 1981, pp. II-80 to II-102.

2.20 Hodulak, L. and Blavel, J.G.," Application of Two Approximate Methods for Ductile Failure Assessment," Elastic-Plastic Fracture: Second Symposium, Volume II - Fracture Resistance Curves and Engineering Applications, ASTM Special Technical Publication 803, October 1981, pp. II-103 to II-114.

2.21 Marston, T.V., Et. al, "Development of a Plastic Fracture Methodology for Nuclear Systems," Elastic-Plastic Fracture:

Second Symposium, Volume II - Fracture Resistance Curves and Engineering Applications, ASTM Special Technical Publication 803, October 1981, pp. II-115 to II-132.

2.22 Turner, C.E., "A Review of Elastic-Plastic Fracture Design Methods and Suggestions for a Related Hierarchy of Procedures to Suit Various Structural Uses," Analytical and Experimental Fracture Mechanics," Sijthoff and Noordhoff, Alphen aan den Rijn, The Netherlands, 1981, pp. 39-58.

2.23 Shih, C.F. and Needleman, A., "Fully Plastic Crack Problems, Part I: Solutions by a Penalty Method and Part II: Application of Consistency Checks," Journal of Applied Mechanics, Vol. 106, ASME, March 1984, pp. 48-64.

2.24 Yagawa, G., Kashima, K. and Takahashi, Y., "A Round-Robin in Finite Element Elastic-Plastic Stable Crack Growth Analysis," Aspects of Fracture Mechanics in Pressure Vessels and Piping, PVP-Vol. 58, ASME, July 1982, pp. 175-184.

2.25 Watanabe, T., et. al, "J-Integral Analysis of Plate and Shell Structures with Through Wall Cracks Using Thick Shell Elements," Paper G/5 3/8, SMIRT, August 1983, pp. 257-264.

2.26 Dodds, R.H. and Reed, D.T., "Elastic-Plastic Response of Tensile Panels Containing Short Center Cracks," Computational Fracture Mechanics - Nonlinear and 3-D Problems, PVP-Vol. 85, ASME, June 1984, pp. 25-34.

2.27 Jung, J. and Kanninan, M.F., "Analysis of Dynamic Crack Propagation and Arrest in a Nuclear Pressure Vessel Under Thermal Shock Conditions," Aspects of Fracture Mechanics in Pressure Vessels and Piping, PVP-Vol. 58, ASME, July 1982, pp. 91-108.

2.28 Yong, C.F. and Palusamy, S.S., "VCE Method of J Determination for a Pressurized Pipe Under Bending," Aspects of Fracture Mechanics in Pressure Vessels and Piping, PVP-Vol. 58, ASME, July 1982, pp. 143-157.

2.29 Schmitt, W., "Three-Dimensional Finite Element Simulation of Post-Yield Fracture Experiments," Computational Fracture Mechanics - Nonlinear and 3-D Problems, PVP-Vol. 85, ASME, June 1984, pp. 119-131.

2.30 Bakker, A., "On the Numerical Evaluation of the J-Integral," Paper G/F 2/4, SMIRT, August 1983, pp. 181-189.

2.31 Cells, A., Squillani, A. and Milella, P.P., "Experimental and Numerical Evaluation of J Integral on Tubes," Paper G/F 4/2, SMIRT, August 1983, pp. 275-281.

2.32 Beliczey, S. and Hofler, A., "Calculations to Experimental Results of Crack Growth," Paper G/F 4/9, SMIRT, August 1983, pp. 329-335.

2.33 de Lorenzi, H.G., "3-D Elastic-Plastic Fracture Mechanics with ADINA," Computer and Structures, Vol. 13, 1981, pp. 613-621.

2.34 de Lorenzi, H.G., "On the Energy Release Rate and the J-Integral for the 3-D Crack Configuration," International Journal of Fracture, Vol. 19, 1982, pp. 183-193.

2.35 ANSYS Engineering Analysis System User's Manual, Swanson Analysis System, Inc., Houston, PA, (Version 4.1c) 1984.

2.36 Rolfe, S.T. and Bersom, J.M., Fracture and Fatigue Control in Structures, Englewood Cliffs: Prentice-Hall, 1977.

2.37 De Castro, P.M.S.T., "R-Curve Behavior of a Structural Steel," Engineering Fracture Mechanics, Vol. 19, No. 2, 1984, pp. 341-357.

2.38 Shih, C.F., et. al, Methodology for Plastic Fracture, Electric Power Research Institute, EPRI NP-1735, March 1981.

2.39 Blejwas, T.E., Woodfin, R.L., Dennis, A.W. and Horschel, D.S., "Containment Integrity Program," NUREG/CR-3131/1, SAND83-0417, March 1983.

3. SEQUOYAH CONTAINMENT

3.1 Previous Results

As listed in Sec. 1.1, three regions have been selected in the Sequoyah containment as locations at which through cracks could develop and leakage occur. The results of previous analyses, summarized here, have indicated that high strains occur in these regions:

- Containment shell, near springline. The maximum membrane strain at 60 psi is greater than 0.0025 in the 1/2-inch plate (Fig. 3.1). The results were obtained from an axisymmetric approximation to the containment [3.1].

- Penetration at Elev. 767', AZ. 260°. A three-dimensional finite analysis [3.1] has shown that the maximum membrane strain for this penetration is about 0.003 at 60 psi (Fig. 3.2).

- Equipment hatch sleeve. A membrane strain of about 0.004 occurs in the 3-inch plate in the sleeve and in the 1 1/2-inch reinforcement of the Sequoyah equipment hatch assembly (Fig. 3.3), according to a three-dimensional finite element analysis [3.2].

3.2 Postulated Crack

Following Sec. 2.1 and Fig. 2.1, an initial surface crack is postulated in each of these regions. It is not clear what is a most realistic crack shape and size. Probably a sensitivity study of different possibilities should be done. For this study, the crack is assumed to be long and shallow, i.e., ECPT case in Sec. 2.4.1. With reference to ASME acceptance standards for radiographed welds in containment vessels [3.3], this is a linear indication with length limits, ℓ, as listed in Fig. 3.4. Since ℓ/a is greater than 3 for linear indications, the maximum crack depth, a, is also listed.

3.3 Surface Crack to Through Crack Propagation

The maximum depth surface crack listed in Fig. 3.4 is postulated to occur in each of the high strain regions of Figs. 3.1, 3.2, and 3.3, as listed in Table 3.1. As described in Sec. 2.4.1, this case is approximated by a flat plate in plane strain with an edge crack (ECPT). Using the analytic solutions summarized in Sec. 2.4.2 for this case, the calculated value of the applied J can be obtained for various levels of nominal true strain (as was done in Fig. 2.4 for the CCP case). Using the Ramberg-Osgood constants for the true stress-true strain curve in Fig. 2.9, the applied J values were obtained for a crack depth of 1/8 the thickness and plotted in Fig. 3.5. The Turner values are representative and easier to calculate and, hence, will be used in the following.

The J resistance of the material is probably the most uncertain quality in this analysis but the bounds presented in Sec. 2.5 and listed as J_R in Table 3.1 are appropriate. Upon setting the applied J values (Eqs. 2.9 and 2.10) equal to the material resistance J_R, the nominal strain ε_R for surface crack propagation is found and listed in Table 3.1. Returning to the pressure versus membrane strain curves in Sec. 3.1, the pressure p_R corresponding to the strain ε_R is obtained for each of the three high strain regions. The pressure p_R represents the pressure at which the postulated surface crack propagates to a through crack and leakage begins. Note that the previous analyses were not extended to sufficiently high strains so as to permit determination of other than a lower bound to p_R. However, one can note that, because of the "flattening" of the pressure versus strain curves, the relative uncertainty in p_R will not be as large as the uncertainty in J_R.

3.4 Propagation of Through Crack

The results of the previous section (Table 3.1) indicate that the postulated surface crack will become a through crack at some pressure beyond 65 psi. One area, the 1/2-inch plate at springline, was selected for further study--both to extend the analyses into the high strain regime so that the p_R in Table 3.1 can be refined and also to estimate the extent to which the through crack will propagate. In this regard, the finite element model illustrated in Fig. 3.6 was formulated. The model includes the 1/2-inch plate near the Sequoyah springline and extends into the hemispherical head and into the 5/8-inch plate below (refer to elevations in Fig. 1.1). Stringers and rings are included in the model and the material properties of Table 2.1 and Fig. 2.9 are used. Symmetry boundary conditions are imposed on both vertical boundaries. The top boundary is constrained in the tangent plane of the hemisphere, but permitted free motion perpendicular to this plane. The meridional forces induced by pressure loading are applied to the lower boundary, which is constrained to move uniformly in the vertical direction. Internal pressure loading is applied to the shell elements which represent the containment shell. A total of 308 elements and 158 nodes are included in the model.

As illustrated in Fig. 3.6, the finite element model has provisions for a 12-inch and 72-inch crack. Phantom elements, as described in Sec. 2.4.3, are associated with each of these cracks.

During the first phases of loading, there is no crack in the model. The pressure is increased from zero in increments and the analysis was accomplished using the slow dynamic approach described in Sec. 2.4.3. At each load increment, the load was increased and then held constant over periods of time equal to 1 and 3 seconds, respectively. An initial integration time step size of 0.001 second was specified. During the solution, this time step size was changed automatically by the program according to third derivative of the displacement (see Sec. 2.4.3). At a pressure of 78 psi, the maximum membrane strain in the entire model was 6.5 percent. This occurred in the 1/2-inch plate at

Elev. 783' 5/8". Figures 3.7 and 3.8 are plots of the maximum membrane strain and the radial displacement at Elev. 783' 5/8" (see Fig. 3.6). Figure 3.9 shows the deformation along a meridian at different pressure levels.

At a membrane strain of 6.5 percent, the postulated surface crack (Table 3.1) is assumed to propagate through the 1/2-inch plate forming a crack with a length of 12 inches. The node at the center of this crack was released and the solution was continued at a pressure level of 78 psi until a converged solution was reached. Using the VCE method as described in Sec. 2.4.3, the value of the applied J was calculated as about 120 k in/in^2. This is much larger than any conceivable J-resistance of the material. One must conclude, therefore, that at a pressure of 78 psi, a through crack of 12 inches will continue to propagate in the meridional direction in the 1/2-inch plate.

The solution was continued to investigate whether this crack would be arrested at the 5/8-inch plate below and the ring above at Elev. 788' 5/8". A 72-inch crack was simulated by releasing all nodes along the left vertical edge in the 1/2-inch plate between these elevations. The solution was continued until convergence. Again, the VCE method was implemented and an applied J of 3860 k in/in^2 was calculated. Again, this unrealistically high value of J indicates the crack will continue to propagate through the ring stiffeners at the top and the 5/8-inch plate at the bottom, i.e., there will be an overall failure.

Note that only one cracking sequence has been studied in this work. If, for example, the postulated surface crack was assumed to propagate through the 1/2-inch plate at a membrane strain of, say, 1 percent (about 60 psi), the resulting through crack could possibly have been arrested.

3.5 References

3.1 Greimann, L., Fanous, F. and Bluhm, D., "Reliability Analysis of Containment Strength," NUREG/CR-1891, August 1982.

3.2 Greimann, L., Fanous, F. and Bluhm, D., "Sequoyah Equipment Hatch Seal Leakage," NUREG/CR-3942, Final Report, February 1985.

3.3 ASME Boiler and Pressure Vessel Code, ASME, Section III, Subsection NE, Class MC Components, Paragraph NE 5320.

4. SUMMARY

The rate of release of radioactive materials from a containment during a severe accident has a significant impact on the consequences of the accident. One hypothesis for a containment leakage model states that the containment will develop a controlled, relatively small leak before the pressure reaches the point where a general rupture of the shell occurs. Another hypothesis states that an overall failure will occur with total release of the vessel contents almost instantaneously. As part of the Containment Performance Working Group (CPWG) and other studies, the Sequoyah ice condenser containment vessel has been studied for some time to predict the possible location and extent of leakage which could occur during a severe accident. In this work, three critical high strain locations were studied to predict crack propagation from an initially small defect.

Several criteria are presented in the literature for predicting crack growth in highly ductile materials such as containment steels. The J integral approach is adopted herein. In simple idealized cases, the J-applied value is given by curve-fits of numerical results that have been developed by others. In this work, a virtual crack extension method for calculating J has been developed for use with a general purpose finite element programs. The various methods are compared herein. Approximate values of the material J-resistance are tabulated.

An initially small surface flaw is first postulated in each of the critical high strain regions. By comparing the J-applied value to the J-resistance, the pressure at which this surface crack propagates is estimated for each of these regions. The 1/2-inch plate near the Sequoyah springline is then selected for further study. A detailed finite element model of the region was prepared and analyzed with the ANSYS program. The pressure in the model was increased up to 78 psi which produced a maximum membrane strain of 6.5 percent. At this point the surface crack was assumed to propagate through the plate and leakage began. Using the virtual crack extension method, two through cracks with different lengths were found to be unstable at this pressure.

4.1 Conclusion

If the critical membrane strain is about 6.5 percent, the Sequoyah containment vessel will begin to leak at about 78 psi. The resulting through crack will not be stable and general failure will occur with the almost instantaneous release of the vessel contents.

4.2 Recommendation

This study should be considered very preliminary. Elastic-plastic fracture mechanics has clearly been pushed beyond the acknowledged state-of-the-art. However, the above conclusion for this application will, most likely, not change.

Table 2.1 Typical Steel Properties, Sequoyah A516, Gr.60

Plate Thickness	σ_y(ksi)	σ_u(ksi)	% elong.	CVN @ -30°F(ft-lb)
7/16"	48.3	66.0	25	N.A.
1/2"	47.3	66.6	33	N.A.
5/8"	49.2	68.3	29	240
1"	46.6	62.0	N.A.	N.A.
1 1/4"	45.5	N.A.	N.A.	N.A.
1 1/2"	45.5	67.1	28	N.A.
3"	42.0	62.0	34	57
Specification	32.0	60-80		30

N.A. - Not Available

Table 3.1 Surface Crack to Through Crack Propagation

Location	Plate Thickness	Crack Depth	J_R k in/in^2	ε_R	p_R
Springline	1/2"	0.083"	3.0 ± 1.0	9 ± 3%	> 65 psig
Penetration	5/8"	0.083"	3.0 ± 1.0	8 ± 2%	> 65 psig
Hatch	1 1/2"	0.17"	2.5 ± 0.5	4 ± 1%	> 82 psig
Sleeve	3"	0.25"	1.5 ± 0.5	2 ± 1%	> 82 psig

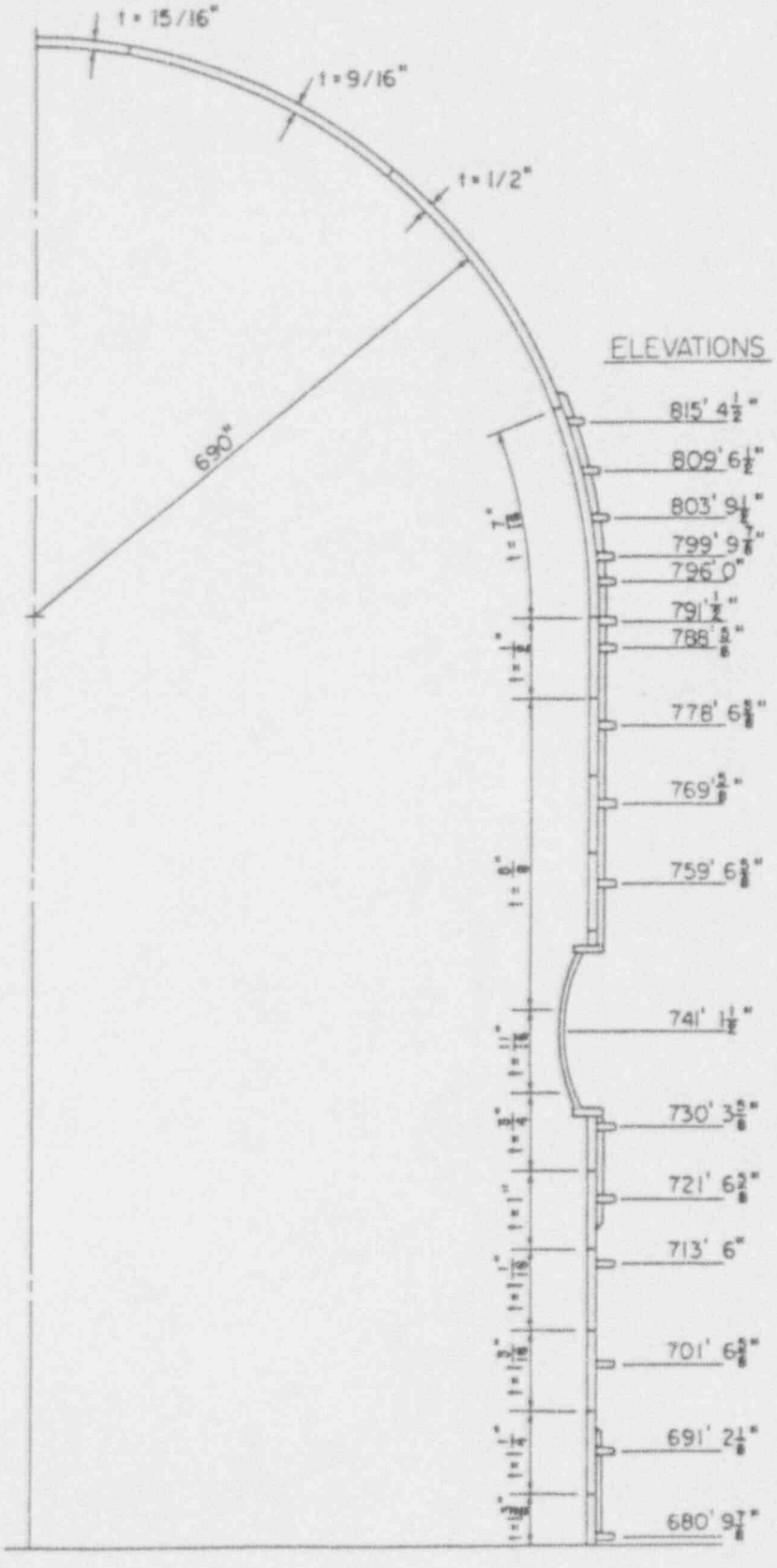

Figure 1.1 Sequoyah Containment - Azimuth 285°

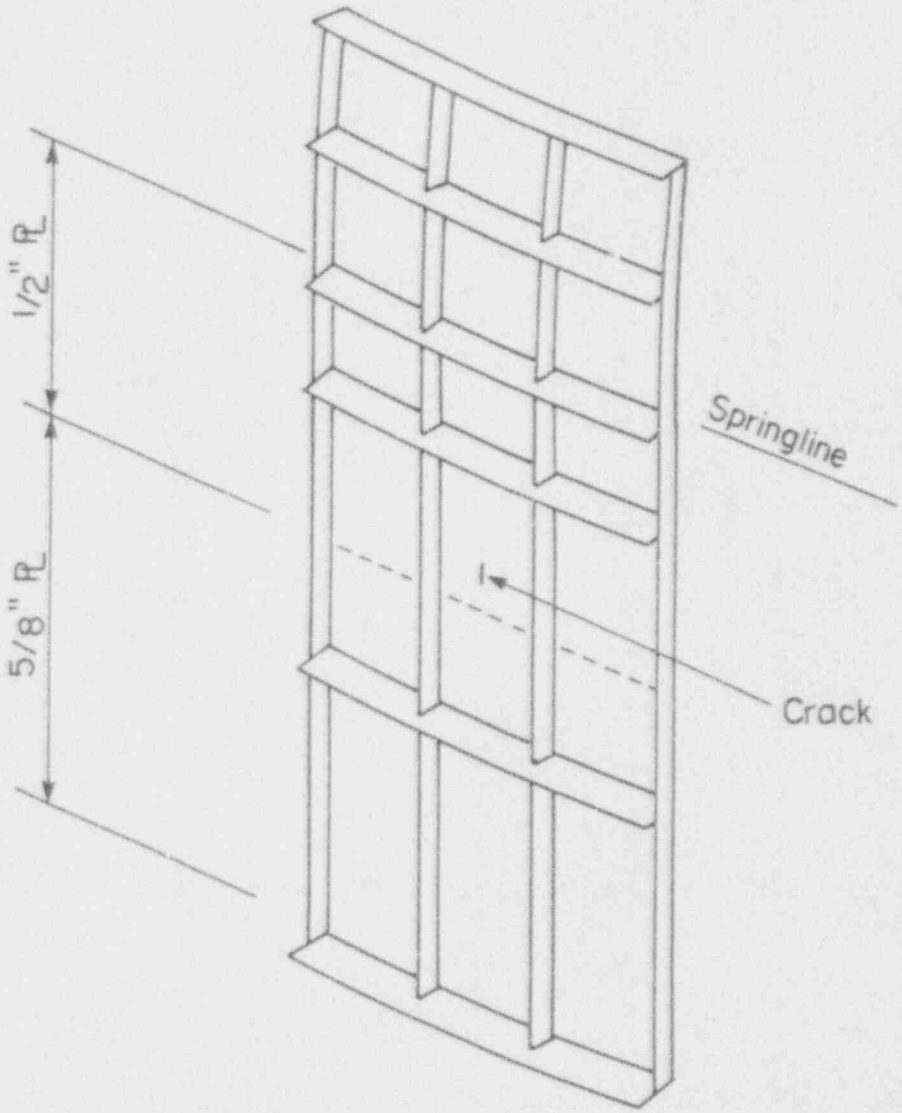

Figure 1.2 Crack in 1/2-inch Plate Near Springline of Sequoyah Containment

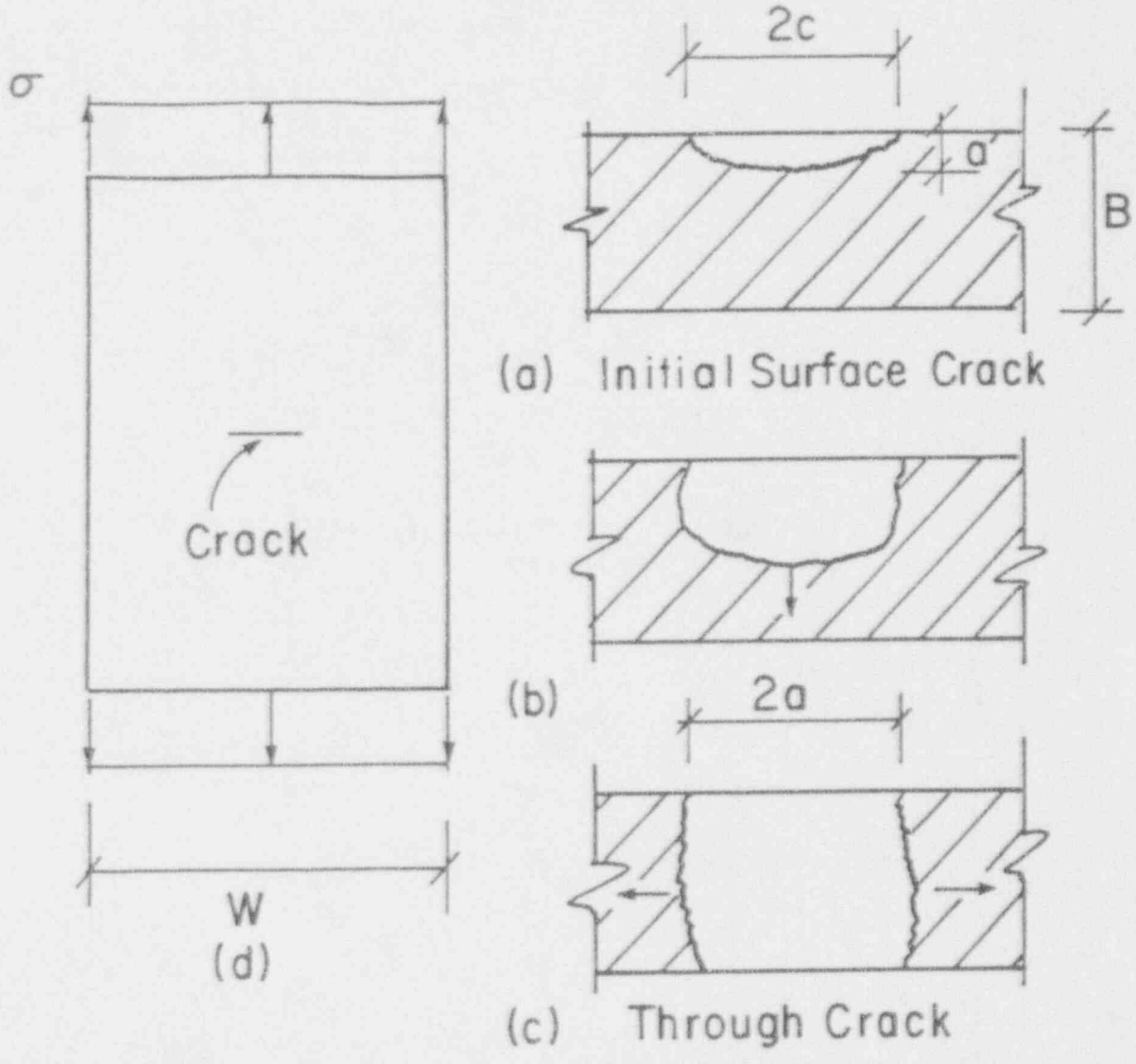

Figure 2.1 Idealized Crack Growth Process

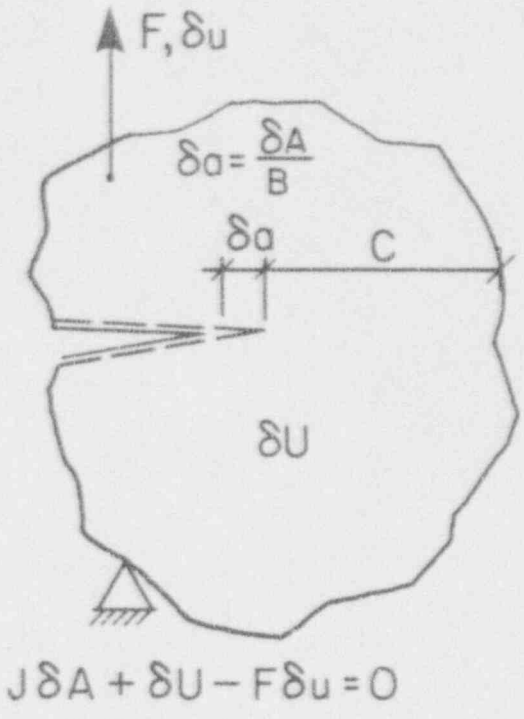

Figure 2.2 Definition of J as Generalized Force for Crack Movement

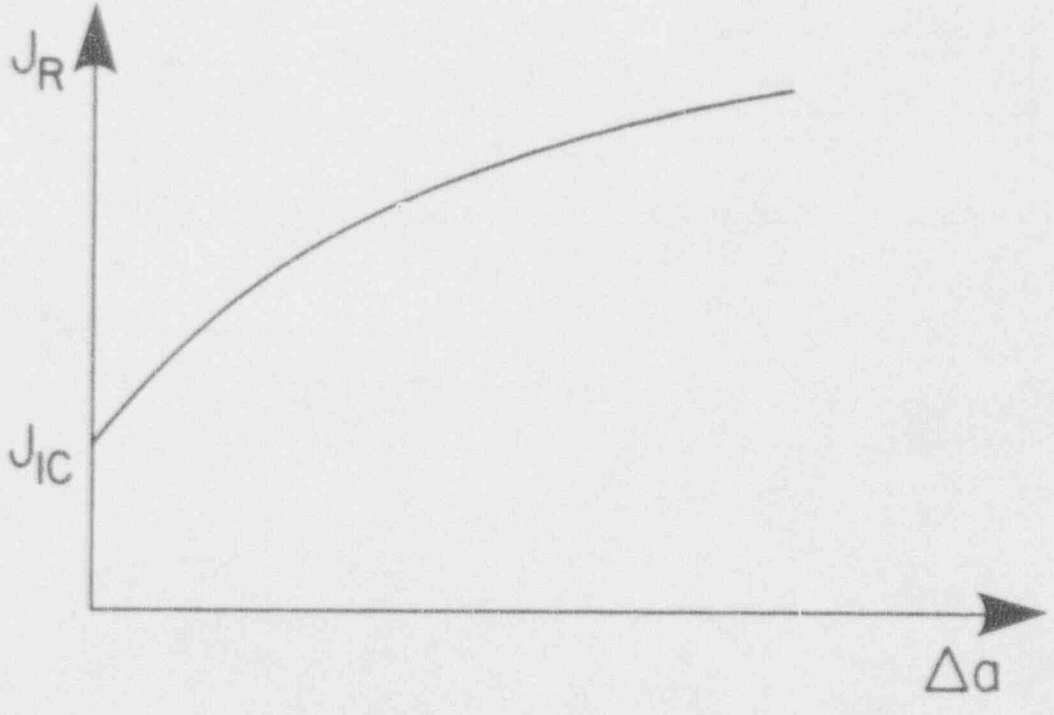

Figure 2.3 Material Resistance to Crack Growth

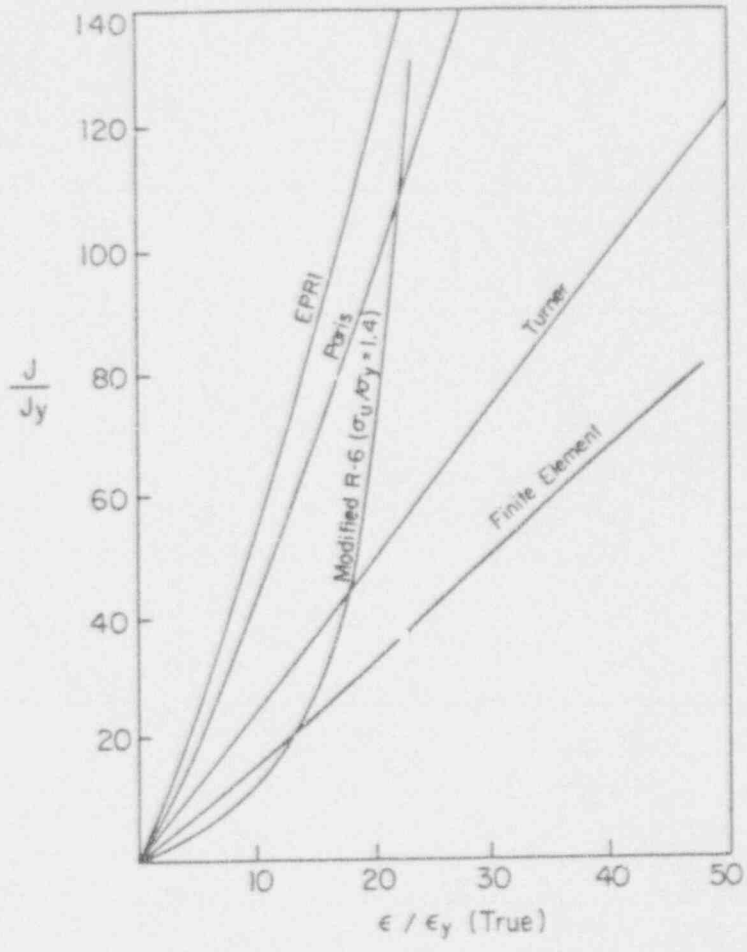

Figure 2.4 Comaprison of J Calculations, Center Cracked Plate (CCP) (a/b = 0.1, α = 1, n = 10)

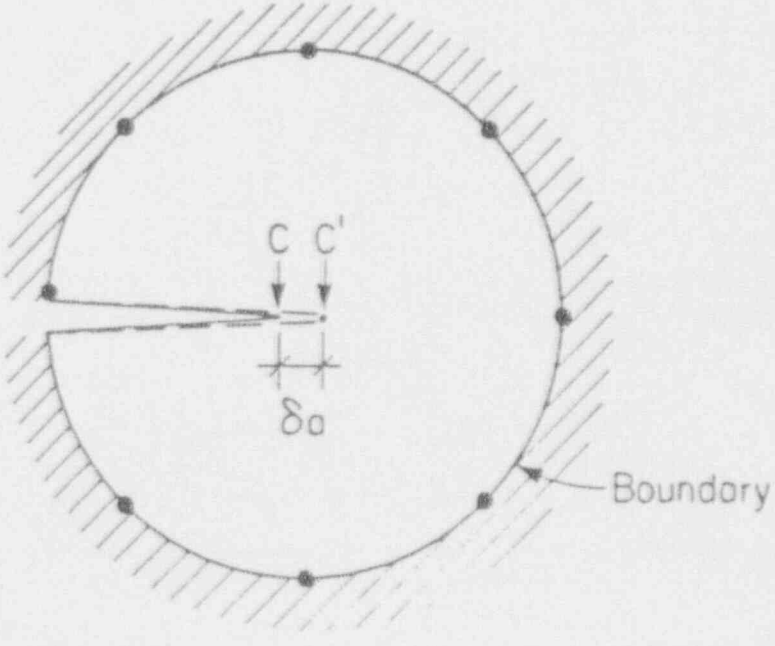

Figure 2.5 Virtual Crack Extension Pattern

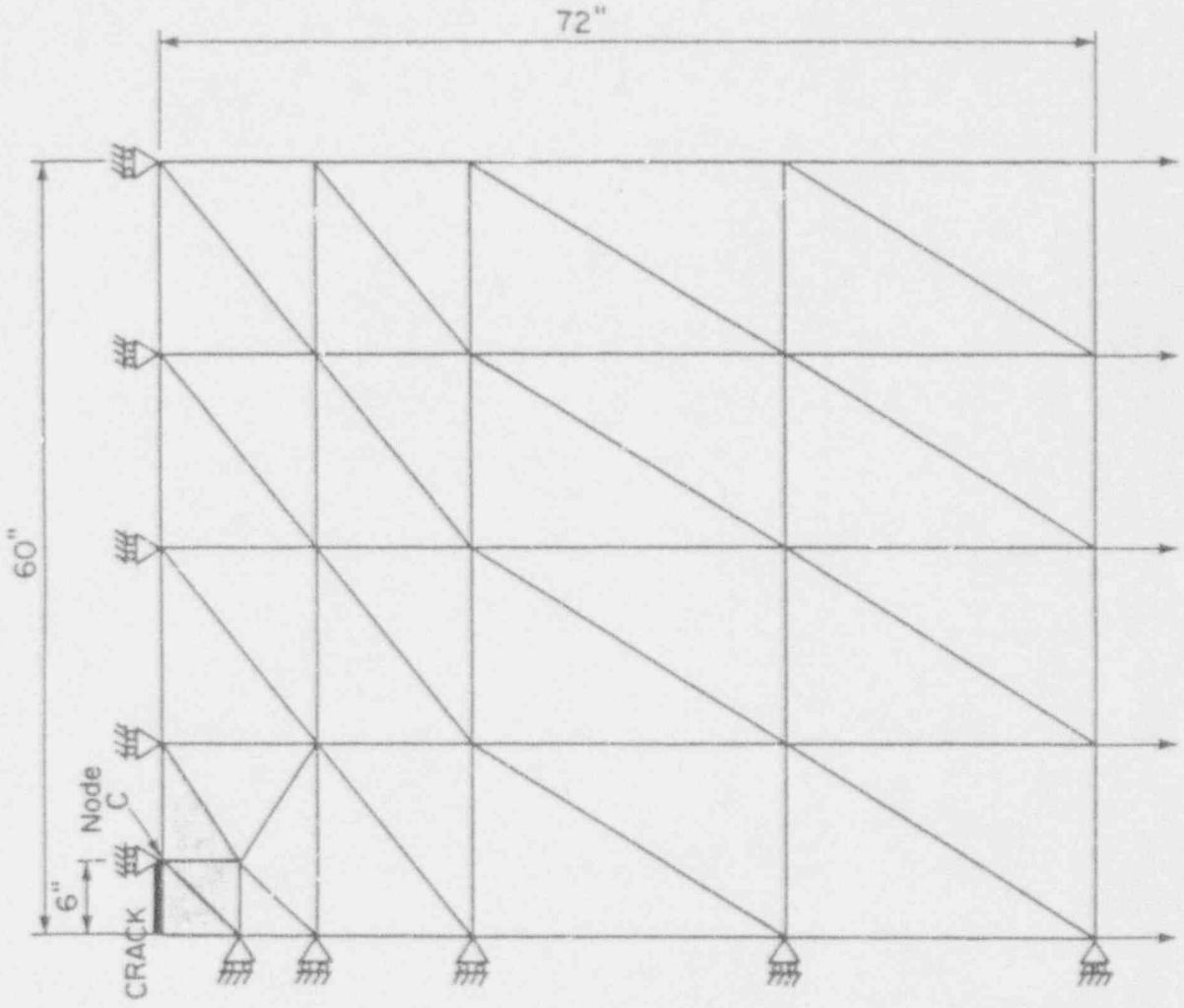

Figure 2.6 One-quarter of Center Cracked Plate, Finite Element Mesh (1/2" Plate, a/b = 0.1, α = 1, n = 10)

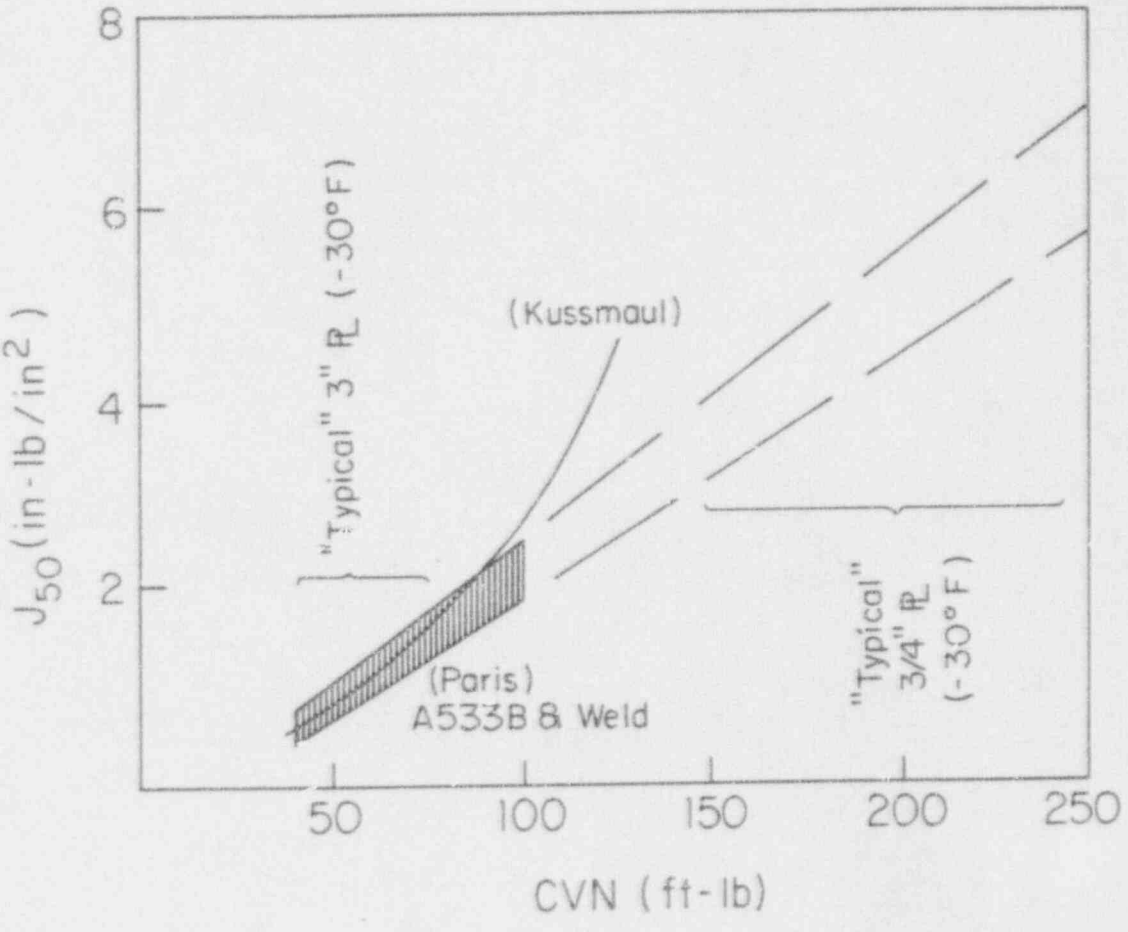

Figure 2.7 Attempted J-CVN Correlation

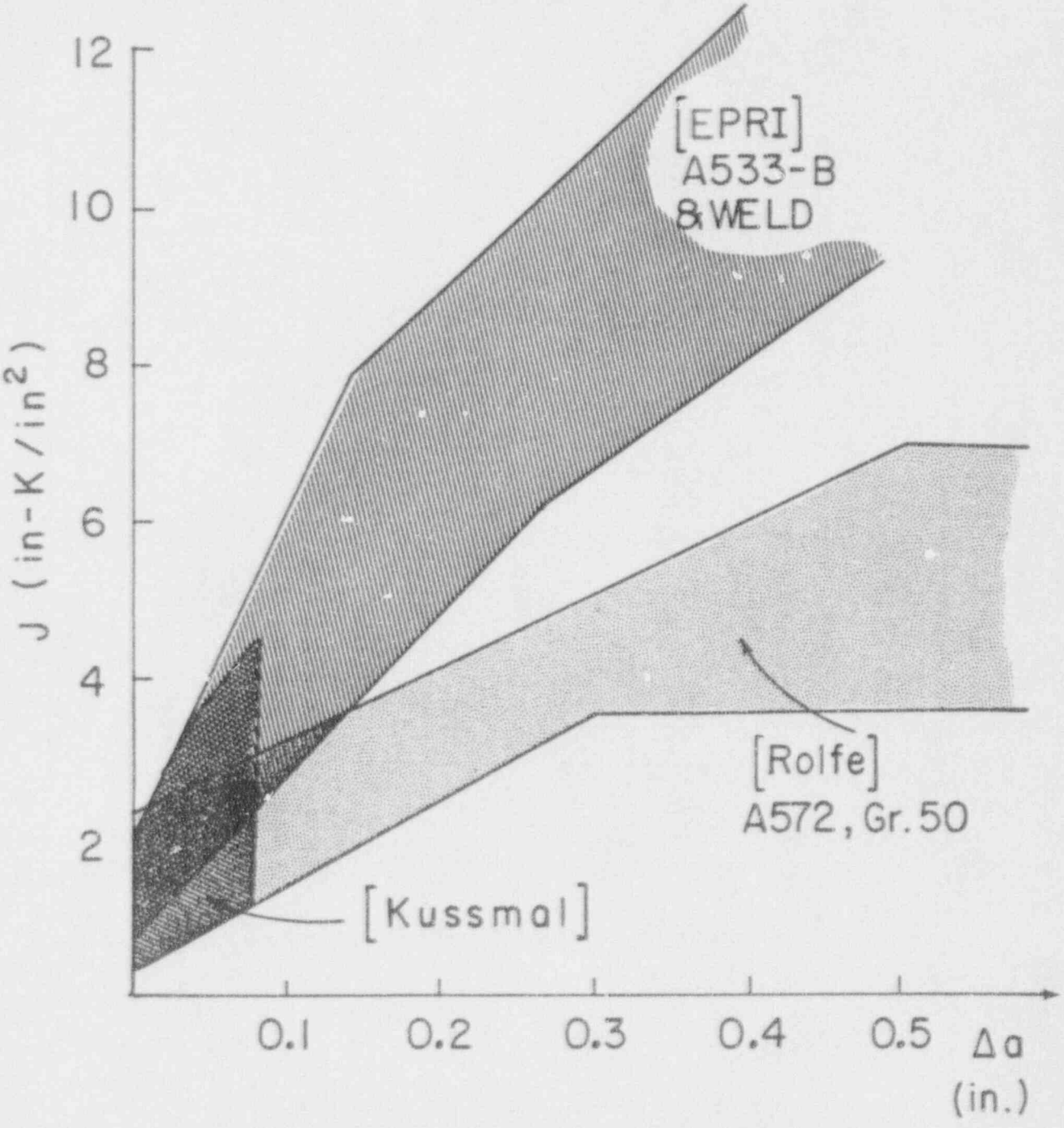

Figure 2.8 Crack Growth Resistance Values

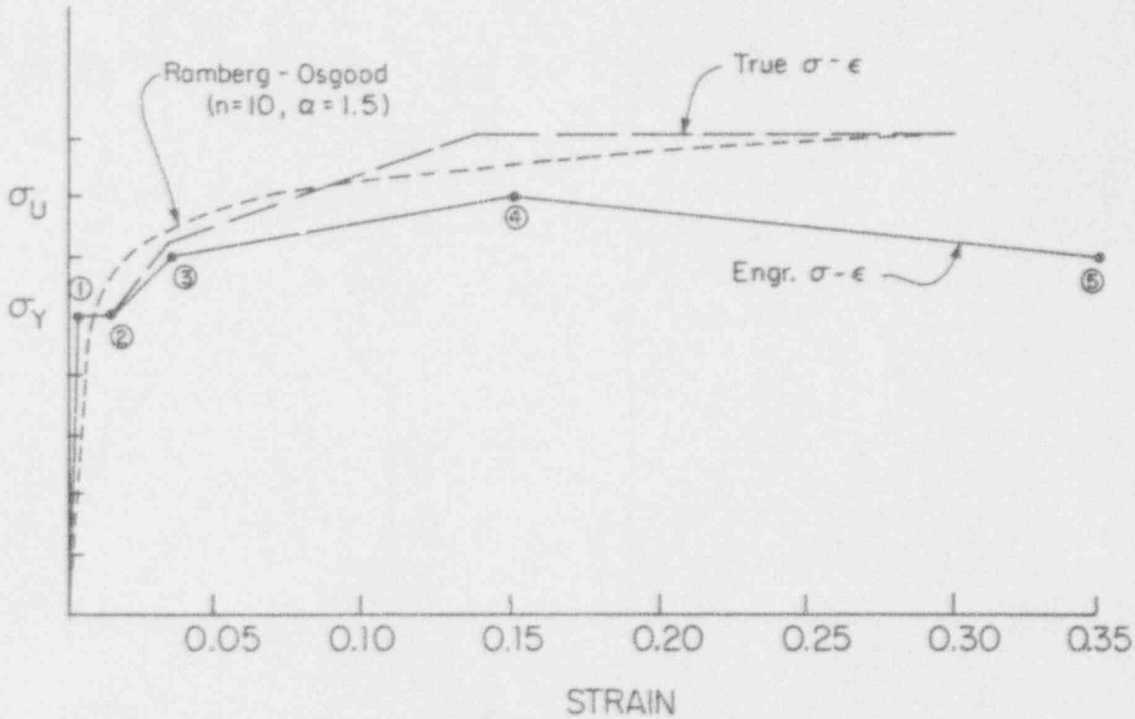

ENGINEERING

Point	ϵ	σ
1	ϵ_Y	σ_Y
2	0.015	σ_Y
3	0.035	$(\sigma_Y+\sigma_U)/2$
4	0.15	σ_U
5	0.35	$(\sigma_Y+\sigma_U)/2$

Figure 2.9 Idealized Stress-Strain Curve for A516, Gr. 60

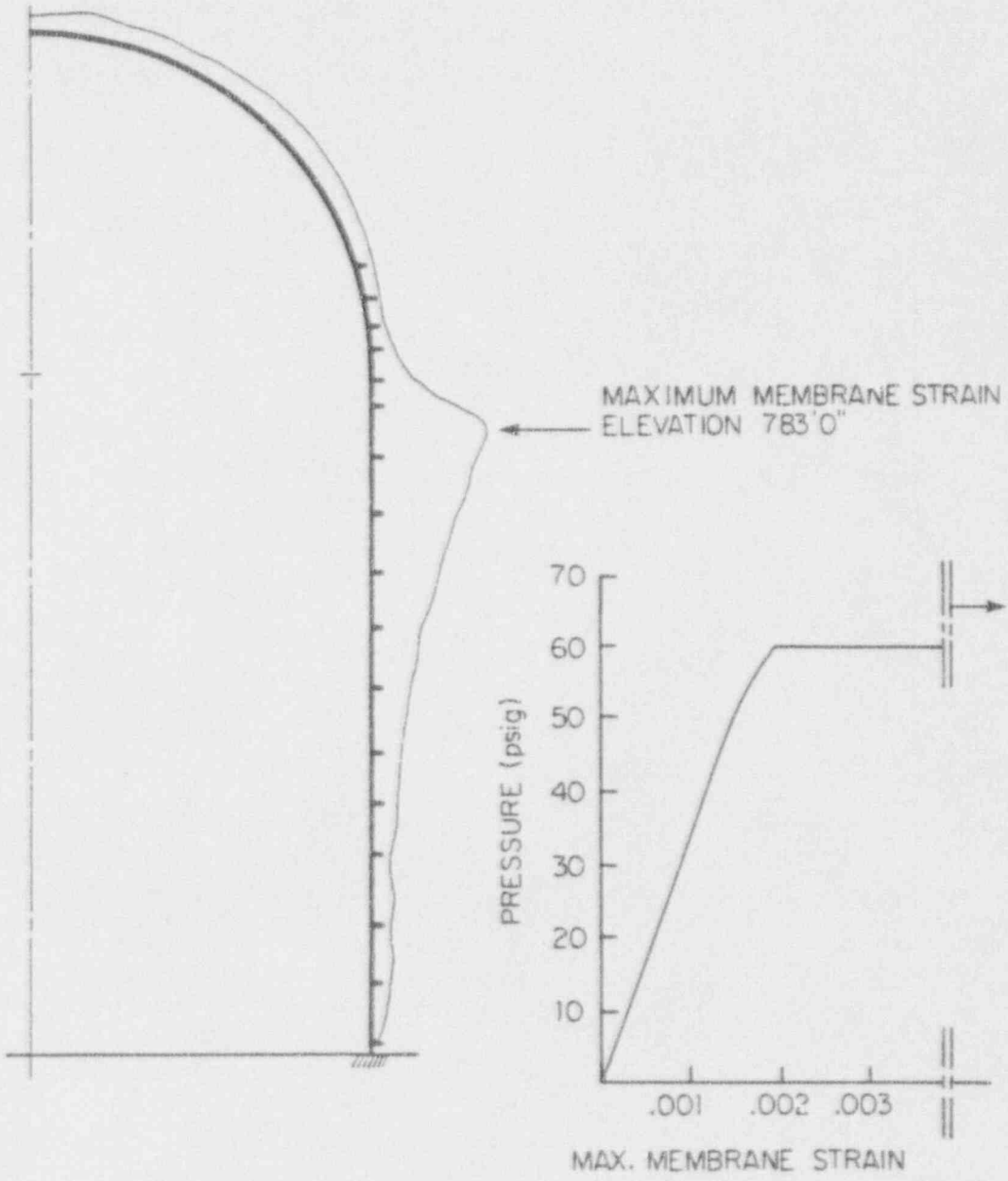

Figure 3.1 Membrane Strain in 1/2-inch Plate Near the Springline of Sequoyah

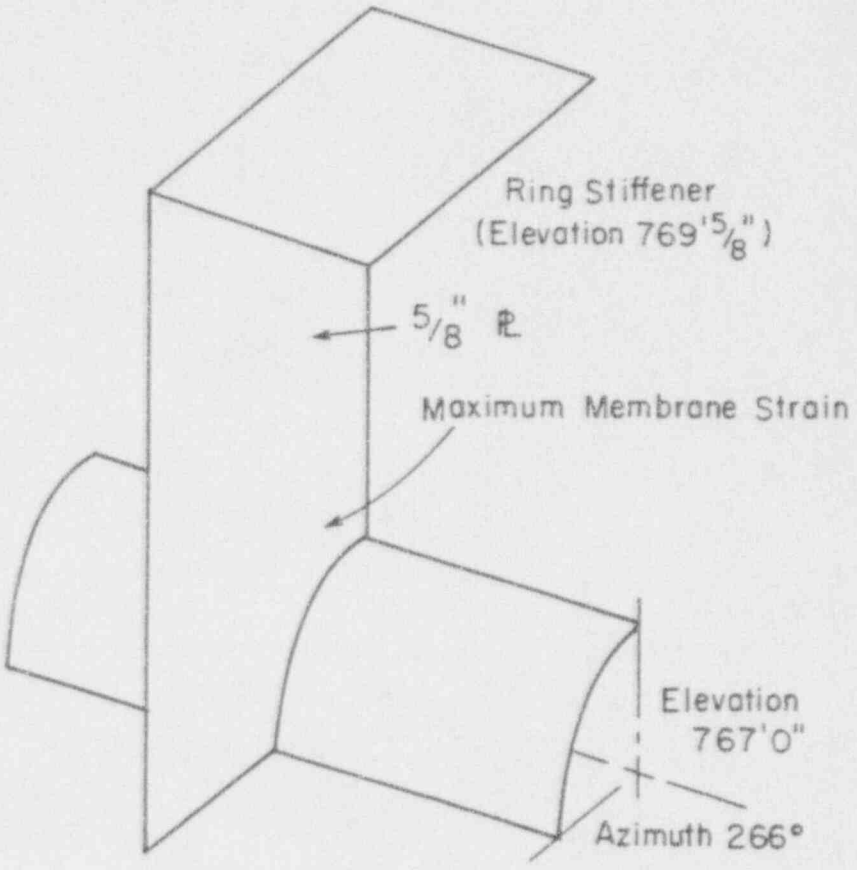

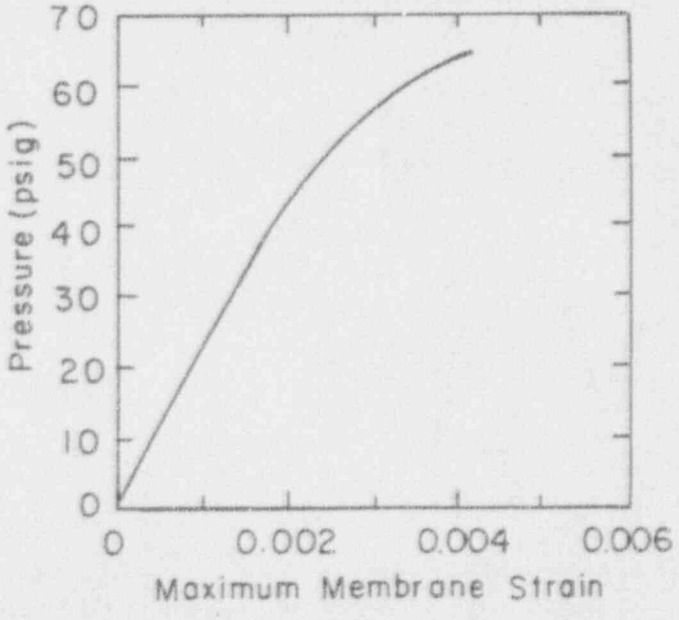

Figure 3.2 Membrane Strain Near Penetration of Sequoyah Containment

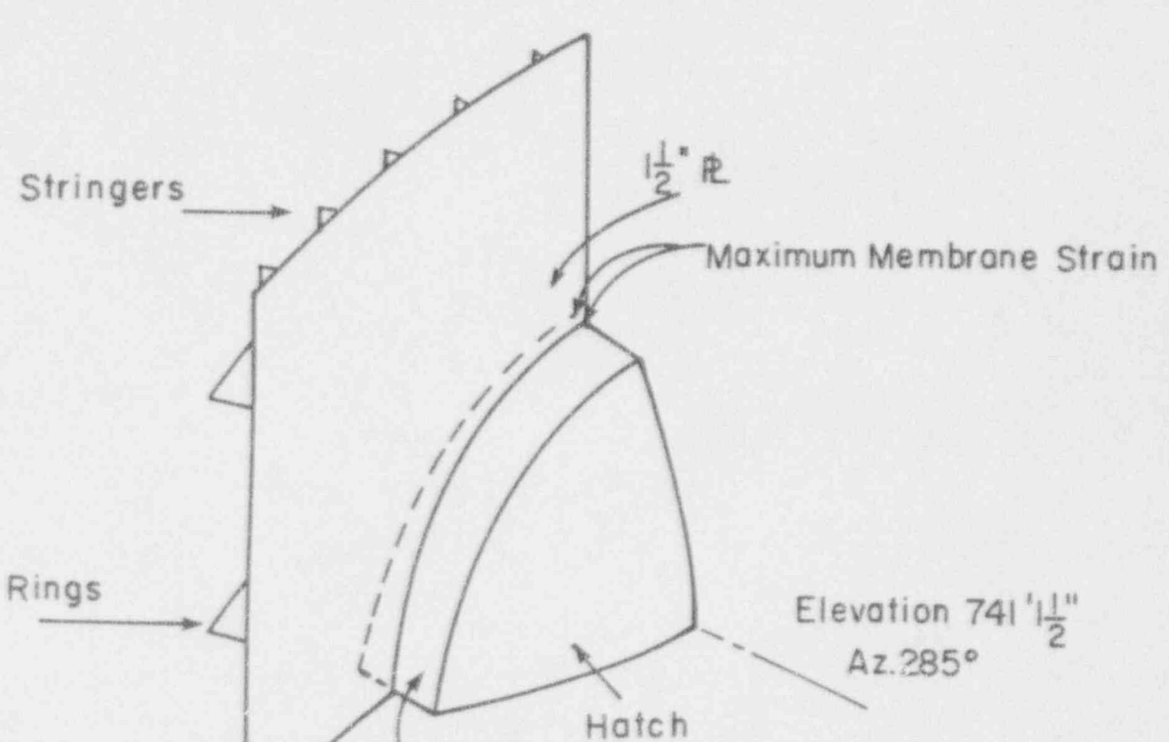

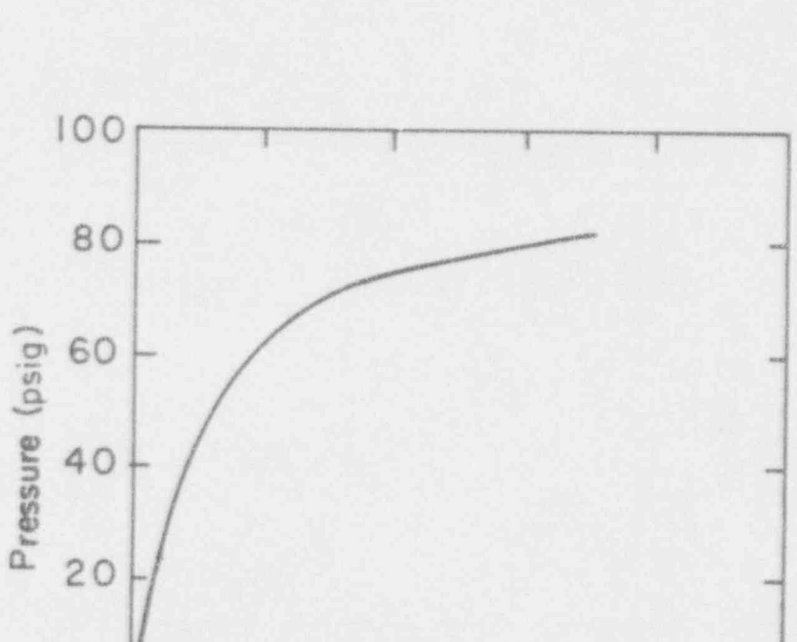

Figure 3.3 Membrane Strain in Sleeve of Sequoyah Equipment Hatch Assembly

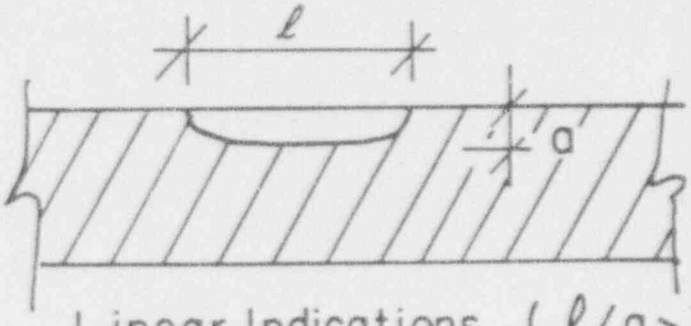

Linear Indications ($\ell/a > 3$)

Thickness	Maximum ℓ	Maximum a
less than 3/4"	1/4"	1/12"
3/4" to 2 1/4"	t/4	t/9
greater than 2 1/4"	3/4"	1/4"

Figure 3.4 ASME Acceptance Standards for Radiograph Welds (Section III, Subsection NE, Class MC Components, Paragraph NE 5320)

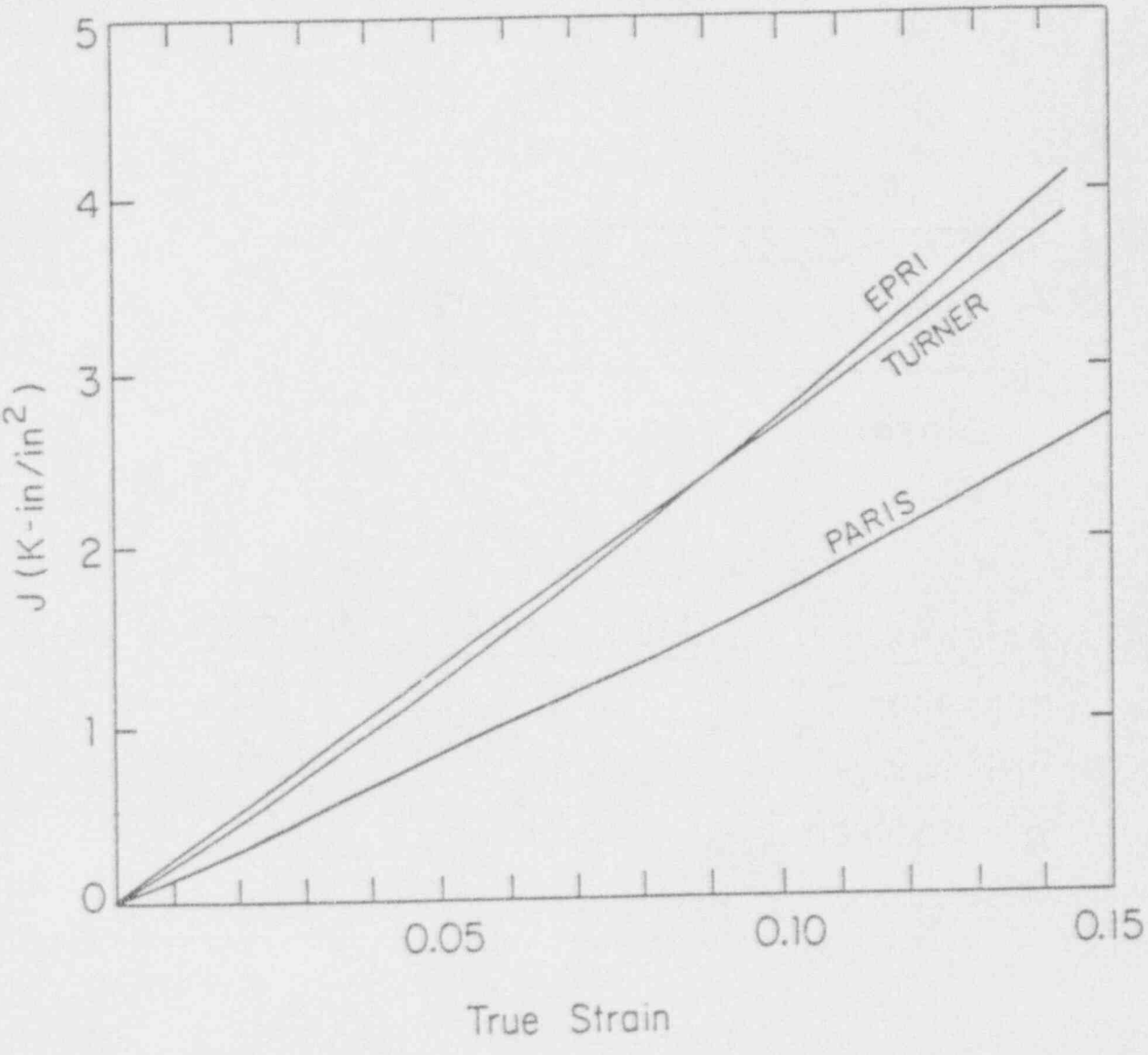

Figure 3.5 Comparison of J Calculations, Edge Cracked Plate (ECPT) (a/b = 1.8, α =1.5, n = 10)

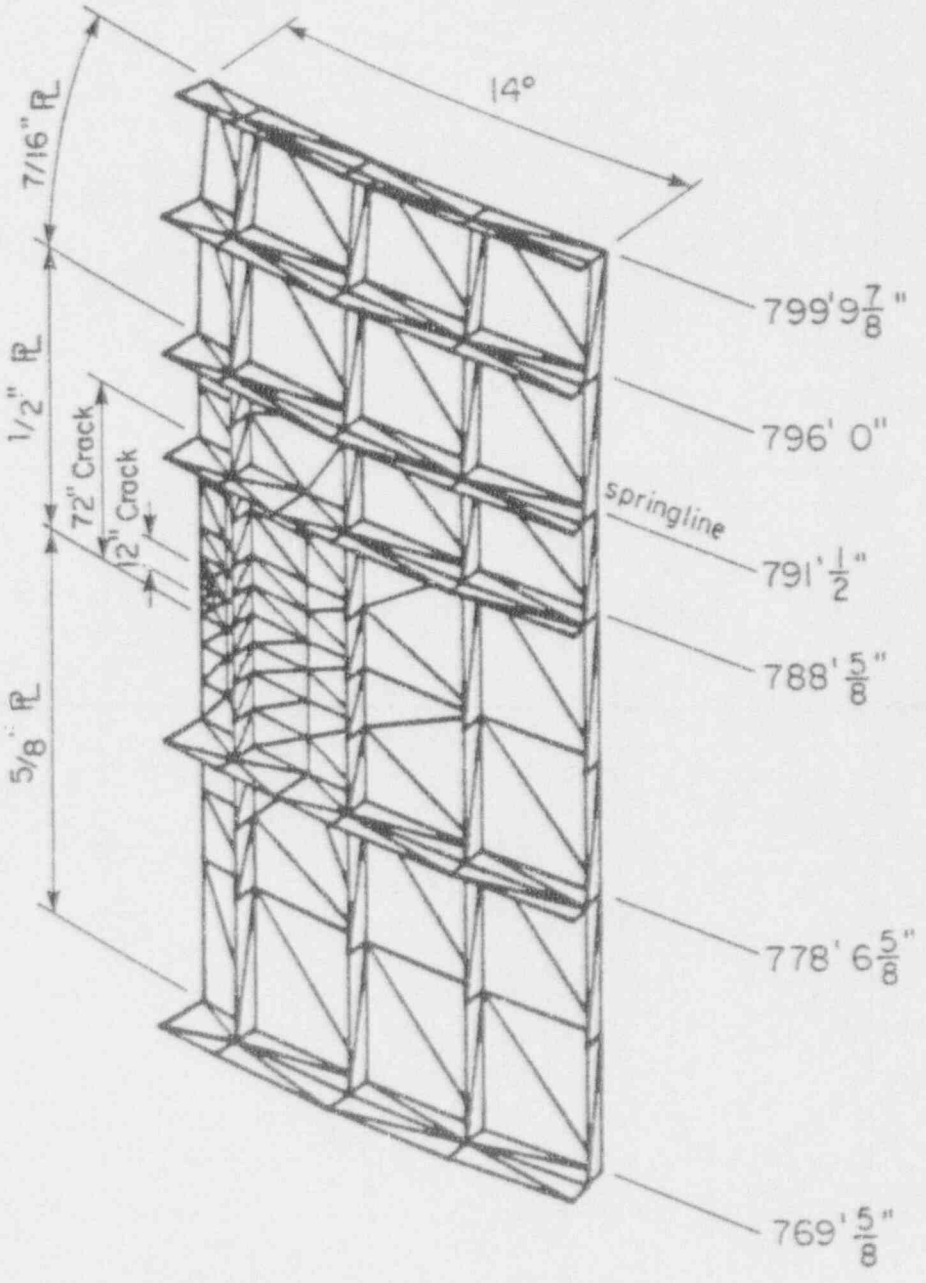

Figure 3.6 Finite Element Model of a Section of the Sequoyah Containment Near the Springline

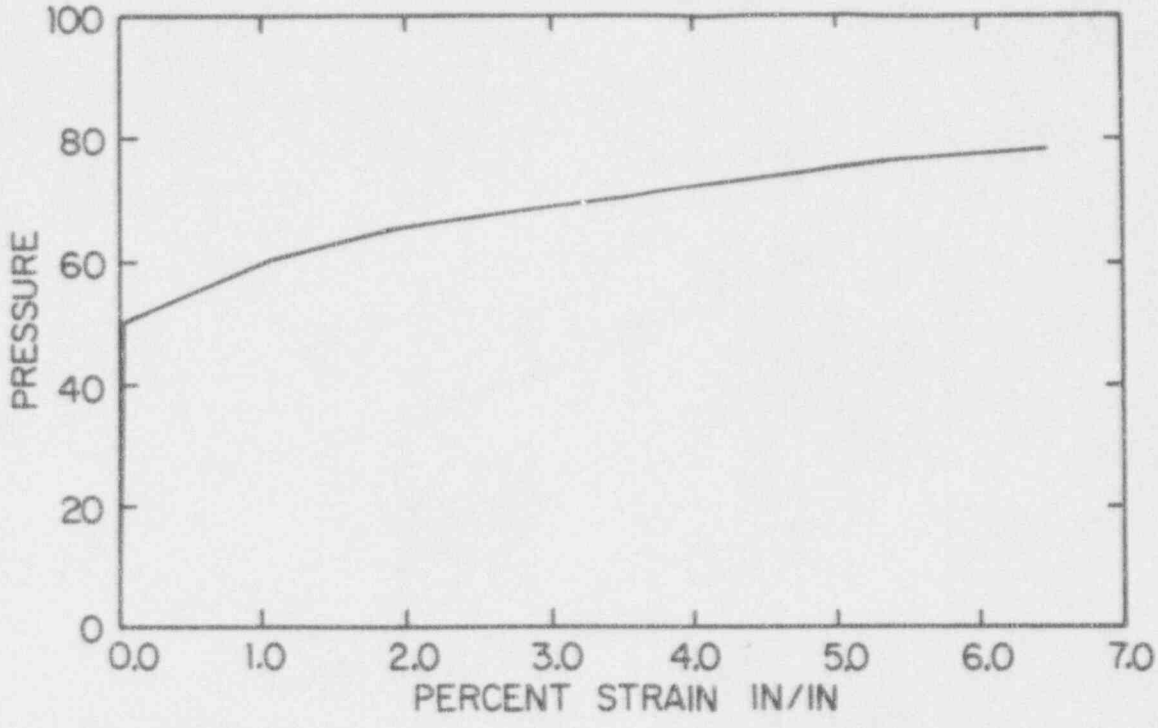

Figure 3.7 Maximum Membrane Strain

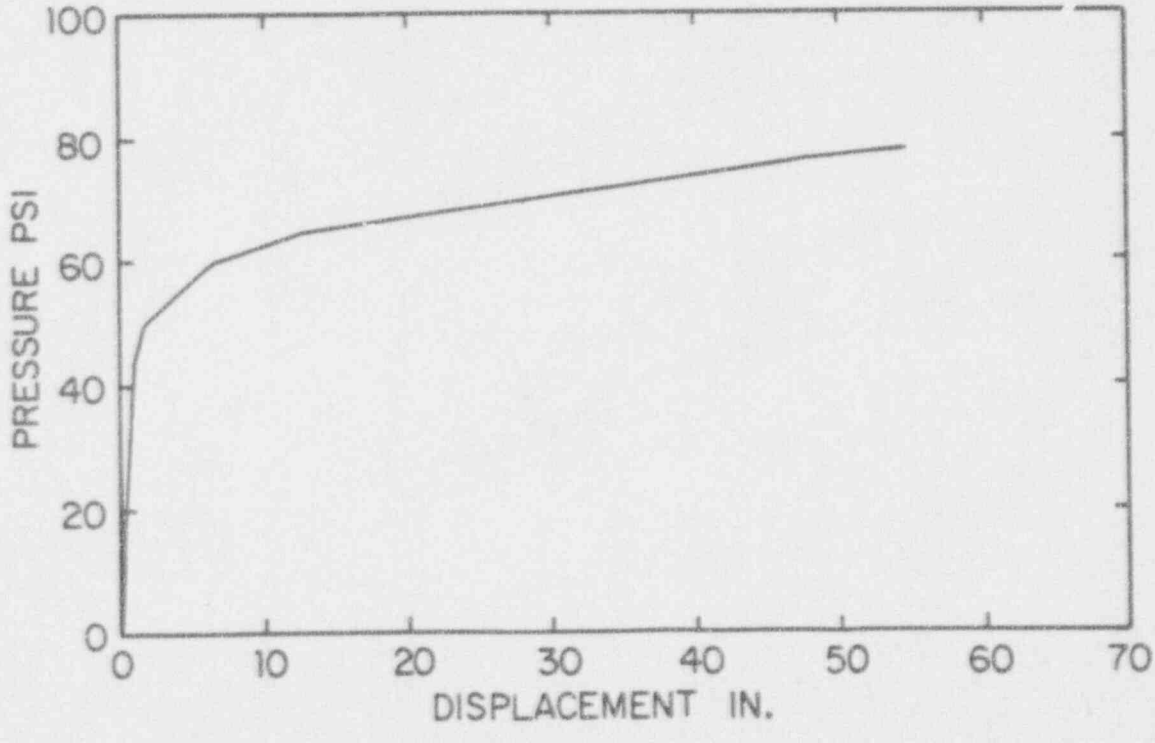

Figure 3.8 Maximum Radial Displacement

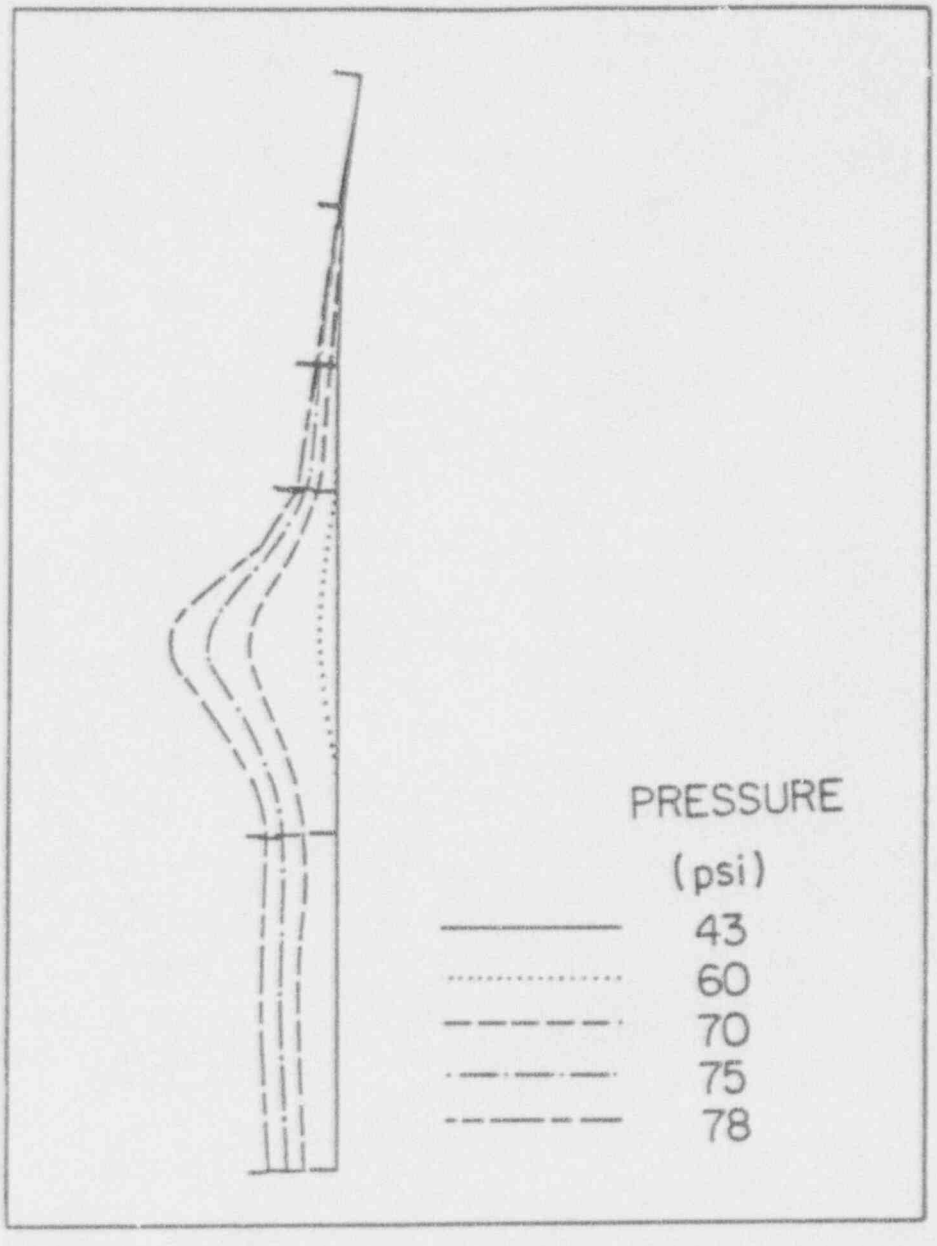

Figure 3.9 Deformed Shape at Different Pressure Levels

NRC FORM 335 (2-89) NRCM 1102, 3201, 3202

U.S. NUCLEAR REGULATORY COMMISSION

BIBLIOGRAPHIC DATA SHEET

(See instructions on the reverse)

1. REPORT NUMBER (Assigned by NRC, Add Vol., Supp., Rev., and Addendum Numbers, If any.)
NUREG/CR-4273
IS-4878

2. TITLE AND SUBTITLE
Crack Propagation in High Strain Regions of Sequoyah Containment

3. DATE REPORT PUBLISHED
MONTH: March
YEAR: 1993

4. FIN OR GRANT NUMBER
A4136

5. AUTHOR(S)
L. Greimann, F. Fanous, D. Bluhm

6. TYPE OF REPORT
Technical

7. PERIOD COVERED (Inclusive Dates)

8. PERFORMING ORGANIZATION – NAME AND ADDRESS (If NRC, provide Division, Office or Region, U.S. Nuclear Regulatory Commission, and mailing address; if contractor, provide name and mailing address.)
Ames Laboratory
Iowa State University
Ames, IA 50011

9. SPONSORING ORGANIZATION – NAME AND ADDRESS (If NRC, type "Same as above"; if contractor, provide NRC Division, Office or Region, U.S. Nuclear Regulatory Commission, and mailing address.)
Division of Engineering
Office of Nuclear Regulatory Research
U.S. Nuclear Regulatory Commission
Washington, DC 20555

10. SUPPLEMENTARY NOTES

11. ABSTRACT (200 words or less)

The rate of release of radioactive materials from a containment during a severe accident has a significant impact on the consequences of the accident. One hypothesis for a containment leakage model states that the containment will develop a controlled, relatively small leak before the pressure reaches the point where a general rupture of the shell occurs. Another states that overall failure will occur with total release of the vessel contents almost instantaneously. The Sequoyah ice condenser containment vessel has been studied for some time to predict the possible location and extent of leakage which could occur during a severe accident. In this work, three critical high strain locations were studied to predict crack propagation from an initially small defect.

The 1/2-inch plate near the Sequoyah springline was selected for further study. A detailed finite element model of the region was prepared and a virtual crack extension method for calculating the J integral was developed for use with the general purpose finite element program. The pressure in the model was increased to 78 psi which produced a maximum membrane strain of 6.5 percent. At this point the surface crack was assumed to propagate through the plate and leakage began. Using the virtual crack extension method, two through cracks with different lengths were found to be unstable at this pressure which would allow almost instantaneous release of the vessel contents.

12. KEY WORDS/DESCRIPTORS (List words or phrases that will assist researchers in locating the report.)
severe accident, containment leakage, Sequoyah ice condensor containment, crack propagation, J integral, finite element

13. AVAILABILITY STATEMENT
unlimited

14. SECURITY CLASSIFICATION
(This Page)
unclassified
(This Report)
unclassified

15. NUMBER OF PAGES

16. PRICE

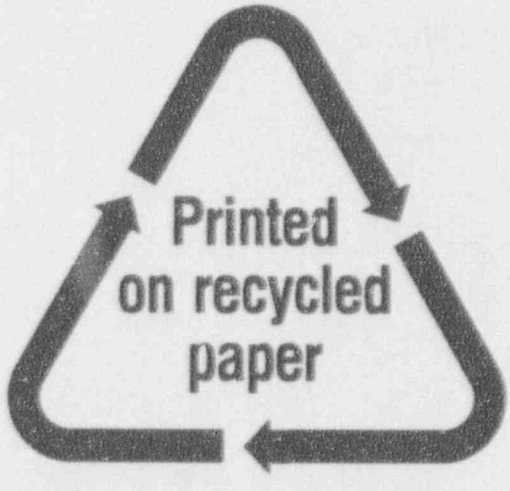

Federal Recycling Program